Annals of R.S.C.B., ISSN:1583-6258, Vol. 25, Issue 4, 2021, Pages. 7968 - 8006
Received 05 March 2021; Accepted 01 April 2021.

Synthesis and Spectral Studies of Some New Complexes Containing Azo Ligand with Anticancer, Antibacterial and Dyeing Performance.

Rehab Abd Al-husseinDabishrehababd1992@gmail.comAlyaaKhideraalyakhider@yahoo.comaalyakhiderDepartment of chemistry ,College of science, university of Baghdad

Abstract

The new designed N,N-bidentateazo ligand 8-[1- (4- sulfonic acid naphtyl) azo] theobromine (SNT), has been synthesized by diazotization and couple for naphthanoic acid and theobromine. The ligand (SNT) was reacted with [Ni(II), pd(II), pt(IV) and Cu(II) to give novel complexes. Both ligand and it's metal complexes were characterized by usual spectroscopic techniques, thermal analysis, magnetic measurement and molar conductance data. The stoichiometric of the complexes were found by mole ratio method and it was (I:2) (M:L) the Ni(II) and pt(IV) complexes found to have octahedral structure while the Cu(II) and pd(II) complexes have distorted octahedral and square planar respectively. The dyeing performance, antibacterial and anticancer activities were investigated for SNT ligand it's complexes.

Keywords: -metal complexes, Theobromine, spectroscopic, anticancer, dying per-Formance

Introduction

The majority of synthesized organic compounds have been influenced by azocompounds because they are particularly fruitful in drugs[1], dyes and cosmetics[2]. These molecules are more soluble than natural dyes at a wide pH ranges and are also thermally stable[3-5].Because of their biological properties, such as antiinflammatory[6] anticancer[7], antibacterial[8] and antifungal[9], azo compounds have been more imperative nowadays. In the world of medicine and pharmacology[10], a terribly significant role is often found to play. Due to their flexible usage in various industrial applications such as coloring fibers[11], they have gained a lot of consideration.

Theobromine, formerly referred to as xantheose by the name 3,7-dihydro-3,7-dimethyl-1H-purine-2,6-dione or 3,7-dihydro-3,7-dimethyl-1H-purine-2,6-dione (3,7-Dimethylxanthine) from theobromacacoa; theo = god, and broma = food; hence, food of the gods [15-16]. Theobromine is the cacao bean's primary alkaloid, which comprises 1.5 to 3 percent of the base and is thus contained in chocolate[17,18]. As a methylated xanthine, theobromine is a potent inhibitor of cyclic adenosine monophosphate phosphodiesterase (CAMP), inhibiting the conversion of the active enzyme phosphodiesterase (cAMP) into an inactive state. In separate metabolic processes, (cAMP) is a second messenger. Theobromine can act as a starting material for the preparation of pentoxifylline, a derivative of methylxanthine. Pentoxifylline increases blood supply and is used for the prevention of vascular dementia and intermittent claudication [19-20].

The present work aims to synthesis and characterize the geometrical structures biological activity and cytotoxicity assay of novel N,N- bidentateligand 8-[1-(4-sulfonic acid naphthyl) azo] theobromine (SNT) and its metal complexes with Ni (II) , Cu (II) , Pd (II) , Pt (IV).

1-MATERAILS AND METHODS

Material and Physical measurements

All the material and solvents were utilized of highest purity. Elemental analyses and metal content for the ligand and its complexes were measured by using (C.H.N.S) was obtained on (Eure EA 3000 Elemental analyzer) and the percentage of metal in complexes

Annals of R.S.C.B., ISSN:1583-6258, Vol. 25, Issue 4, 2021, Pages. 7968 - 8006
Received 05 March 2021; Accepted 01 April 2021.

was done by using a "GBC 933 Plus "Flam Atomic Absorption Spectrophotometer. FT-IR spectrophotometry Fourier Transform Infra-Red spectra were recorded by SHIMADZU 8400s spectrophotometer in the rang (250- 4000) cm-1 with CsI. UV-Vis Spectra for all the studied compounds were recorded on the (SHIMADZU 1800 – UV-Visspectrophotometer) using DMSO in the range of (250-1100) nm. The ^{1}H-NMR spectra were measured on a BRUKER AV 400 Avance -III (400 MHz and 100MHz) instrument with tetramethylsilane as the internal standard. Thermal analysis (TGA and DSC) of the metal content of the synthesized ligands and complexes were determined by utilizing (SDT Q600 V20.9 Build). The melting points for all the compounds were performed by Gallenkamp melting point apparatus. The molar conductivity for metal ion complexes were studied in DMSO (10^{-3} M), which were determined to Hunts Capacitors Trade Mark British made. The chloride contents of the studied complexes were carried out by using Mohr method. The magnetic susceptibility of the studied complexes was performed at room temperature by Auto Magnetic Susceptibility Balance Model Sherwood Scientific. The SEM was performed by (quanta FEG 450).

2-Synthesis of (SNT) ligand

The ligand 8-[1-(4-sulfonic acid naphthyl) azo] thebromine (SNT) Was synthesized according to the method reported in the literature[21] with some modification as was shown in scheme below:-

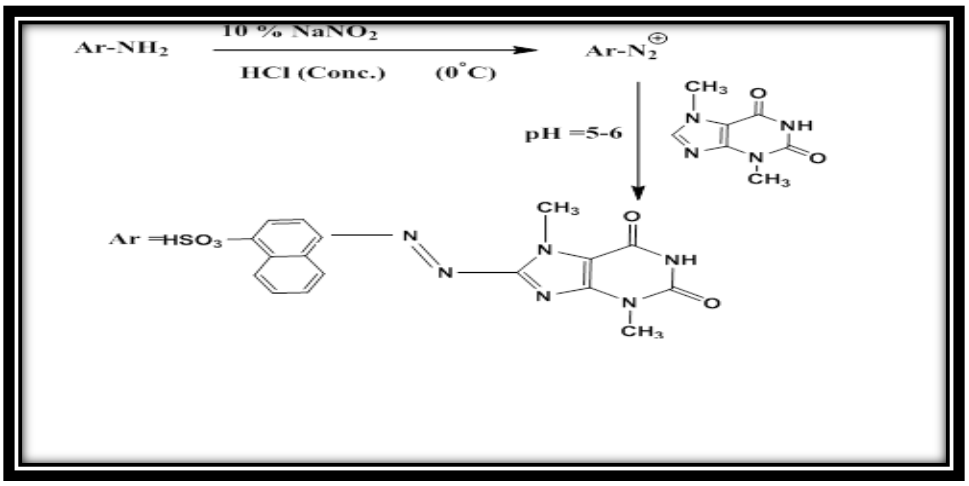

The azo- theobromine ligand was synthesized, via preparation of diazonium salt (0.01 mole, 2.232 gm) of naphthionic acid dissolved in an ice acidic media (10 ml distilled water. and 10 ml conc. HCl). The 10 ml of 10% sodium nitrite was added carefully and dropwise at (0^{o}C). Subsequently the diazonium salt was stirred for (30 min) to complete the diazotation.

The coupling component of theobromine (0.01 mole, 1.801 gm) was dissolved in cold 5 % ethanolic basic solution (KOH). After the diazotation was complete the diazonium salt solution was added drop by drop to alkloide solution of theobromine with stirring at (0^{o}C). The pink precipitate was appeared and the pH value was adjusted to a neutral value (pH = 5-6), then left synthesis of complexes overnight for complete precipitation. After that filtered and washed with (1:1) (ethanol:H_2O) to remove the trace of starting material then dried.

Synthesis of metal complexes

[Ni(II) , pd(II), pt (II) and Cu(II)] complexes were synthesized in a mole ratio (1:2) (M:L) by dissolving of metal chloride (0:237,0.383,0.486 and 0.134) gm. (0.00lM) respectively. An ethanolic solution of the ligand (SNT) [0.828 gm., 0.002M]

Annals of R.S.C.B., ISSN:1583-6258, Vol. 25, Issue 4, 2021, Pages. 7968 - 8006
Received 05 March 2021; Accepted 01 April 2021.

was added gradually while stirring. After that reflexed for (3) hours and the reaction was followed with TLC.

The colored precipitate was filtered off and washed several times with (1:1) (distilled water: ethanol). Finally left dry and collect. Table (1) was appeared the some physicochemical properties and elemental analysis for the ligand (SNT) and it's complexes.

Table(1): physicochemical properties and elemental analysis

Compounds (M.wt) (gm/mol)	Yield (m.p) ℃	Color (λMax) nm	% elementcal analysis experimental (theoretical)						Λm $ohm^{-1}cm$ mol^{-1}
			C	H	N	S	M	Cl	
SNT(C17H14N6O5S) (414.404)	**77.75 (324-326)**	Pale Pink (512)	49.90 (49.22)	3.61 (3.37)	21.79 (20.27)	4.54 (3.86)	---	---	----------
[Ni(C17H14N6O5S) 2Cl2] (958.498)	**76.32 (298-300)**	magneta (520)	43.53 (42.56)	2.55 (2.92)	17.92 (17.52)	6.38 (6.67)	7.19 (6.12)	6.49 (7.40)	2
[Cu(C17H14N6O5S)2Cl2] (963.348)	**83.26 (280-282)**	Green brown (616)	44.06 (43.59)	4.07 (3.11)	12.63 (17.43)	4.37 6.64	6.06 (6.59)	7.36 (7.37)	4
[Pd(C17H14N6O5S)2] Cl2 .H2O (1024.228)	**87.11 (300-302)**	Dark purple (556)	39.65 (39.83)	2.94 (2.73)	16.70 (16.40)	6.55 (6.24)	11.02 (10.39)	6.51 (6.93)	77
[Pt(C17H14N6O5S)2 Cl2]Cl2 .H2O	**86.94 (310-312)**	Dark green	34.85	3.41	14.25	5.80	16.73	11.43	76

3-Result and Discussion

Generally, all complexes were synthesized by reacting the azo ligand (SNT) to the selected metal salts using (1:2) (M:L) mole ratio, while the ligand was synthesized via diazotization naphthenic acid in acidic media and then coupling with alkaloid theobromine as nucleophile All synthesized compounds were colored, which is a general characteristic of azo compound due to trans mutation in the delocalization of electrons[22]. The data was gained from atomic absorption to determine the metal percentage &, chloride percentage by Mohr method and elemental analysis were in satisfactory convention with general formulae was specified for the ligand (SNT) and it's metal complexes. The molar conductivities data in ethanol for [Ni(II) and Cu(II)] complexes are (2and4) $ohm^{-1}cm^{2}$.mol respectively which was indicated non electrolytic nature but regard on[pd(II) and pt(IV)] had (77and 76) $ohm^{-1}cm^{2}$mol^{-1} which were possessed (I:2) electrolytic nature as was abulated in Table 1. Also the proposed structure support by spectroscopicmeasurement (FT-IR, HNMR and UV- Vis) and thermal analysis. The ligand (SNT) and their solid complexes are thermally stable and unaffected by moisture and atmospheric gases

4-Mole ratio

The mole ratio for the ligand (SNT) and its [Ni(II), Pd (II), Pt (IV) and Cu (II)] complexes were explored applying The mole ratio method [23], which it is the most familiar technique utilized toidentifythenatureofthecomplexesformedinsolutionwantingisolation. This

Annals of R.S.C.B., ISSN:1583-6258, Vol. 25, Issue 4, 2021, Pages. 7968 - 8006
Received 05 March 2021; Accepted 01 April 2021.

technique was measured absorbance versus molar ratio of the (M:L) whentheamountoftheligandisvaried(0.25ml)astheamountofthemetal ion is held constant, then the complex was formed and there is no retable dissociation, such a plot affords a sharp break. At this point indicates the composition ofcomplexes.

Figure (1) was shown the relationship between the absorbance and (M:L) ratio while the date was listed in Table (2) .The datareveal(1:2)(M:L)forallsynthesizedcomplexes

Table (2): Absorbance versus mole ratio for SNT-Metal ion in solution

M:L	Absorbance			
	Ni(SNT)	Cu(SNT)	Pd(SNT)	Pt(SNT)
1:0.25	0.00	0.630	0.55	0.25
1:0.50	0.18	0.841	0.73	0.40
1:0.75	0.52	0.930	0.88	0.71
1:1.00	0.75	1.110	1.11	0.89
1:1.25	0.93	1.270	1.30	1.19
1:1.50	1.11	1.360	1.45	1.28
1:1.75	1.25	1.450	1.55	1.49
1:2.00	1.27	1.510	1.61	1.51
1:2.25	1.30	1.530	1.62	1.56
1:2.50	1.33	1.520	1.65	1.58
1:2.75	1.39	1.540	1.66	1.61
1:3.00	1.40	1.501	1.64	1.60
1:3.25	1.44	1.550	1.65	1.61
1:3.50	1.44	1.540	1.62	1.59
1:3.75	1.45	1.560	1.63	1.58
1:4.00	1.40	1.510	1.67	1.59

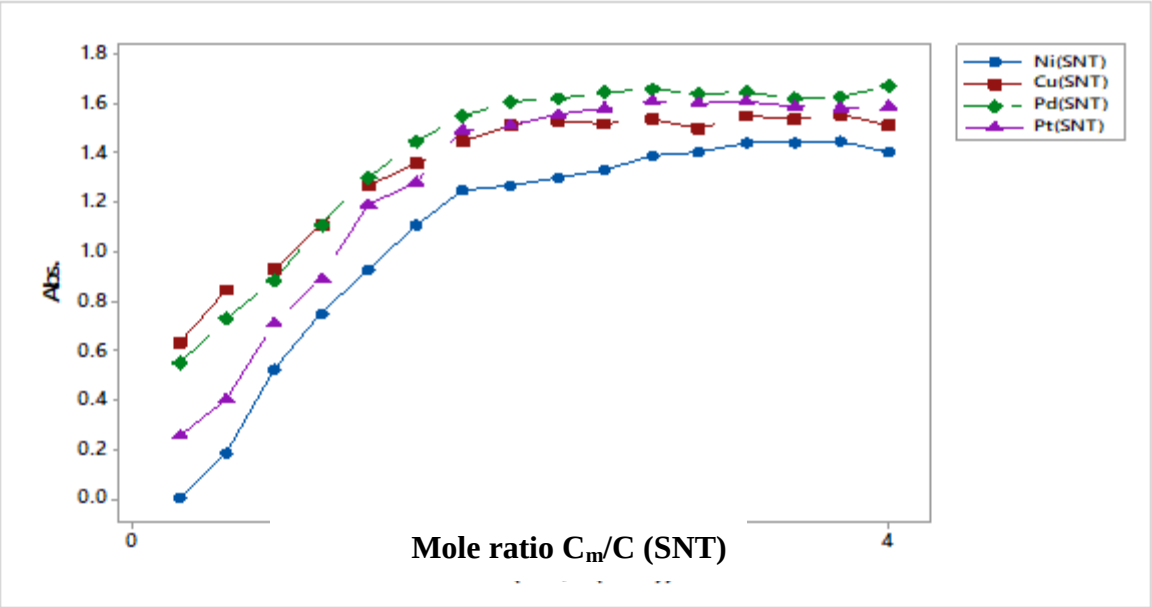

Figure (1): Mole Ratio for the ligand (SNT) and its complexes.

Annals of R.S.C.B., ISSN:1583-6258, Vol. 25, Issue 4, 2021, Pages. 7968 - 8006
Received 05 March 2021; Accepted 01 April 2021.

5-stability constant and Gibbis free energy

Itispossibletofindthestabilityconstantspectrophotometrically.For the Complexes with mole ratio (1:2) (M:L) we use the following equations [24].

$$K = \frac{(1-a)}{4\alpha^3 c^2} \qquad \alpha = \frac{(Am - As)}{Am}$$

While: C=molar concentration of the complexes in molar , c = $10^{-3}M$

α = degree of dissociation

$A_{S=}$ the absorption of solution containing (1:1) stoichiometric (M:L) A_m =the absorption of solution containing (1:2) stoichiometric (M:L)

The above equation can be applied to all synthesized complexesTable (3) collect all the results were obtained .The stability of the complexes as below.

The thermodynamic parameters behavior of ΔG(Gibbs free energy) were also computed from the equation:

$$\Delta G = - RT \ln K$$

Where:

R=gas constant = 8.31 J. mole^{-1}. K

T = absolute temperature (Kelvin)

And we conclude from the results that the retation to synthesis the complexes are spontanous

Table (3): The stability constant (K) and Gibbs free energy (ΔG) for synthesized complexes

Complex	As	Am	K	Log K	ΔG
[Ni(SNT)2Cl2]	0.75	1.27	22.36*10^5	14.6	-36449.07
[Cu(SNT)2Cl2]	1.110	1.510	10525.71	16.16	-39993.22
[Pd(SNT)2] Cl2 .H2O	1.11	1.61	5790339.36	15.57	-1.432
[Pt(SNT)2Cl2]Cl2 .H2O	0.84	1.51	2140131.45	14.57	-36053.21

6-FT-IR

The main target of studying FT-IR spectra is to find out the nature of bonded between the ligand and the metal ion, as well as which of the active groups are affected by chelation when comparing the spectra of metal ions with the spectrum of the free ligand. Which represented by obtaining bands splitting, shifts in band position, intensity change, disappearance of bands and appearance of new bands [25]. The assignments of bonding sites of the ligand (SNT) and its selected metal ions complexes were readily assigned depeneding on comparison with literature data [Table (4)] in cesium iodide

In the FT-IR spectrum of (SNT) (Figure2) Thebandsdetectedat(3458,1695,1670,1550,1485,1456,1432,1397 ,1226and1145)cm^{-1}wereascribedtoυ (NH),υ(C=N),υ(C=C),υ(N=N),υ (C-N=N- C)andυ (SO_3H)respectively,[structure (1)] whilethe FT-IR spectra for [Ni(II), Pd(II), Pt(IV) and Cu(II)] complexes Figures (3-6) and [structure(1-3)] reflected that the SNT acted as a neutral N,N- bidentate ligand chelating *via* nitrogenatomin(N=N)andnitrogenin(C=N)$_{imd.}$toformhexagonalchelatingring. This manner of

Annals of R.S.C.B., ISSN:1583-6258, Vol. 25, Issue 4, 2021, Pages. 7968 - 8006
Received 05 March 2021; Accepted 01 April 2021.

chelation was rein forced by the change in shap and shift to lower wavenumberofbothυ(N=N),υ(C-N=N-C)andυ(C=N)andthepresenceofnewbands at (611-615) cm^{-1} and (509-522)cm^{-1}which related to (M-$N_{imd.}$) and (M- N_{azo})respectively[26].

Moreoverabrodningbandat(3385-3448)cm^{-1}inthespectra of the complexes[Pt$(SNT)_2Cl_2]Cl_2.H_2O$,[Pd$(SNT)_2]Cl_2.H_2O$ due to the presence of lacttice or coordinated water. Generally, lattice water absorb at (3500-3200) cm^{-1} (symmetricandasymmetricυ (OH))[27]. This corresponds to the thermal analysis (TGA) and elemental analysis (C.H.N.S).

Furthermore,inthespectraofallcomplexesthedoubletbandsobserved at(1595-1548)cm^{-1}duetothe$\upsilon(c=o)_{pyrm}$and$\upsilon(NH)_{pyrm}$theyremainsmoreorless at the same position in complexation indicating that they are not a center of chelation.

Finally, the new band at (358-381) cm^{-1} in the complex spectra related to υ(M-Cl)[28].

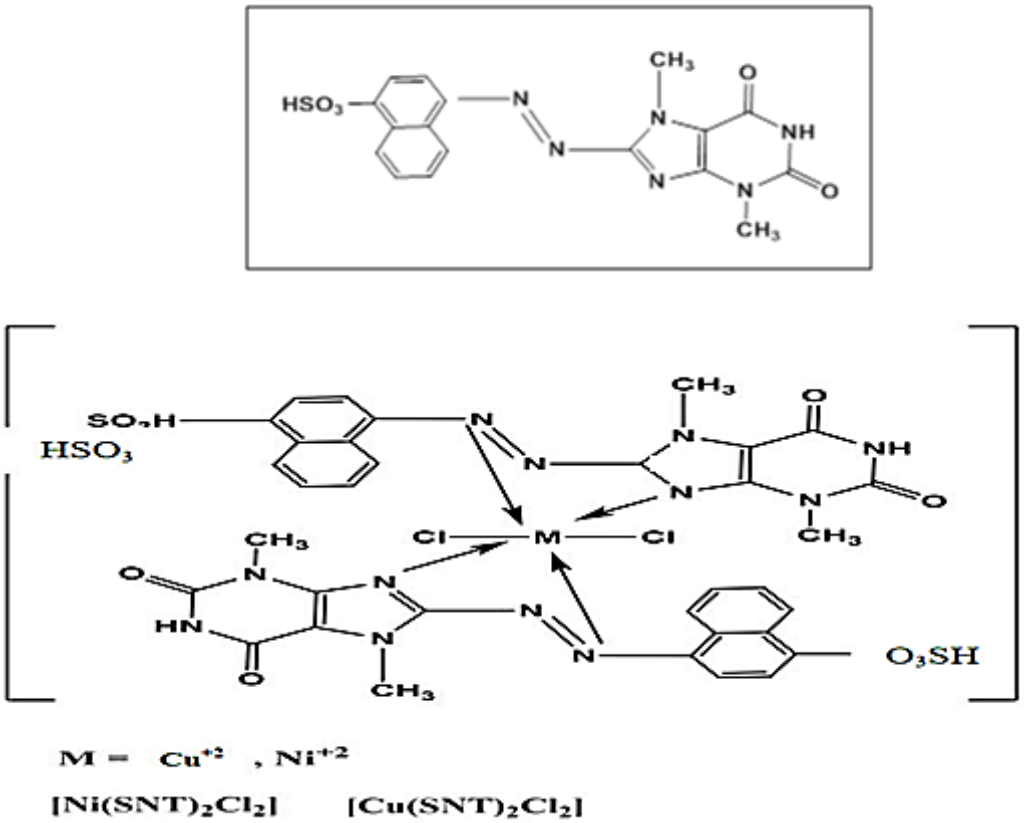

Structure (2)

Annals of R.S.C.B., ISSN:1583-6258, Vol. 25, Issue 4, 2021, Pages. 7968 - 8006
Received 05 March 2021; Accepted 01 April 2021.

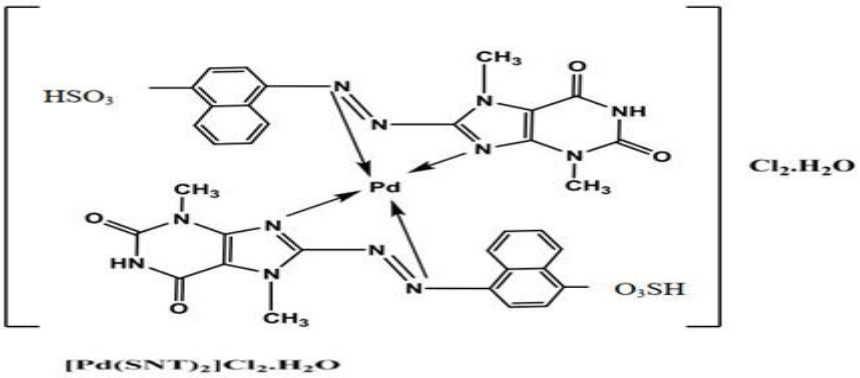

Structure (3)

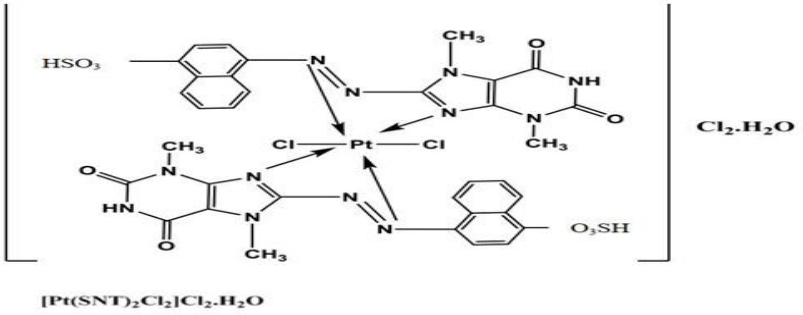

Structure (4)

Table (4) Main spectroscopic FT – IR date for the ligand (SNT) and its complexes

Assessment Center	υ(O-H)$_{H2O}$	υ(N-H)$_{NH\ Pyrm.}$ δ(N-H)	υ(C=N)$_{Im\ d.}$ υ(C=C)$_{na\ ph.}$	υ(C=O)$_{Pyim}$ υ(C=O)$_{ald.}$	υ(N=N)	υ(-C-N=N-C-)	υ(S+aSO$_3$H)	υ(M-N)$_{Imd.}$	υ(M-N)$_{azo}$	υ(M-Cl)	υ(M-O)$_{H2O}$
SNT	--	3458 m 1595 w	1595 d,m 1550 d,m	1695 d 1670 s ---	1485 T,s 1456 T,s 1432 T,s	1397 s	1226 d,s 1145 d,s	---	---	---	H_2O
[Ni(SNT)$_2$Cl$_2$]	---	3398 s 1575 w	1575 d 1550 w	1714 d 1652 s ---	1438 w	1396 d,w 1367 d,s	1218 d,s 1176 d,s	613 m	516 w	337 s	--
[Cu(SNT)$_2$Cl$_2$]	---	3432 m 1595 v.w	1595 d 1550 m	1693 s ---	1458 d 1434 w	1365 w	1222 d,s 1188 d,s	615 m	514 m	370 w	---
[Pd(SNT)$_2$]Cl$_2$ .H_2O	3415 br,m	3449 s 1598 w	1595 d,m 1560 d,m	1708 s ---	1458 d,w 1433 d,w	1404 d,w 1379 d,w	1226 T,s 1203 T,s 1176 T,s	613 m	522 w	358 s	---
[Pt(SNT)$_2$Cl$_2$]Cl$_2$ .H_2O	3448 br. v.w	3440 v.w 1595 v.w	1595 d 1550 m	1691 s ---	1452 d,w 1423 d,w	1365 v.w	1224 d,m 1205 d,m	611m	511 w	368 w	---

Annals of R.S.C.B., ISSN:1583-6258, Vol. 25, Issue 4, 2021, Pages. 7968 - 8006
Received 05 March 2021; Accepted 01 April 2021.

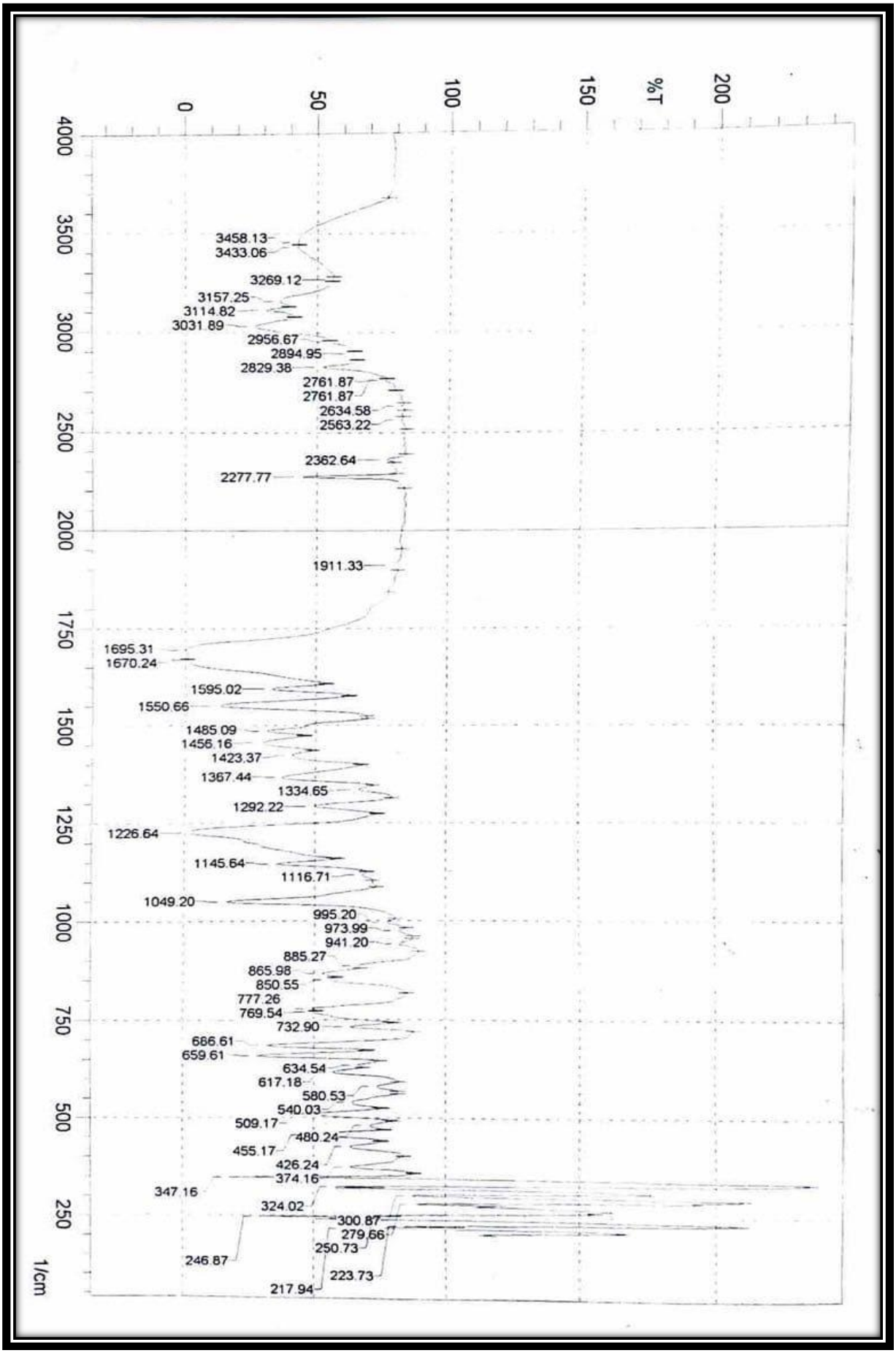

Figure (2): FTIR spectrum of SNT ligand.

Annals of R.S.C.B., ISSN:1583-6258, Vol. 25, Issue 4, 2021, Pages. 7968 - 8006
Received 05

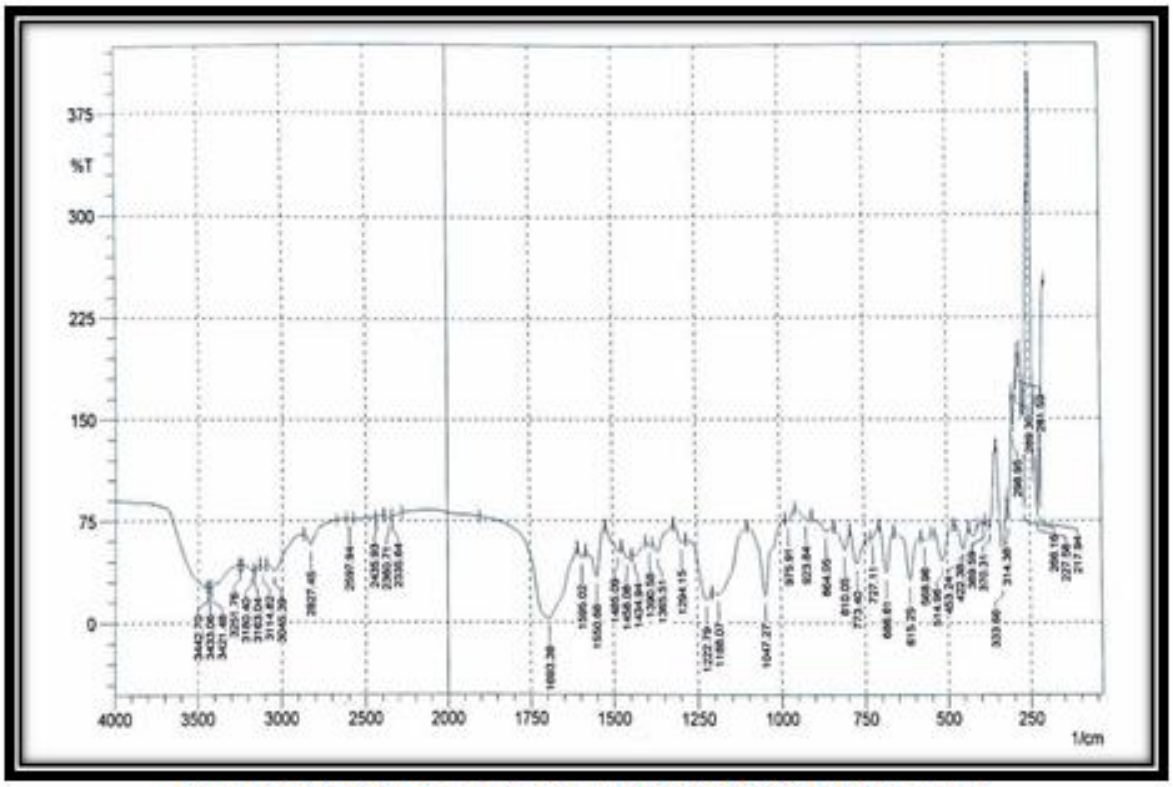

Figure (3): FTIR spectrum of $[Ni(SNT)_2Cl_2]$ Complex.

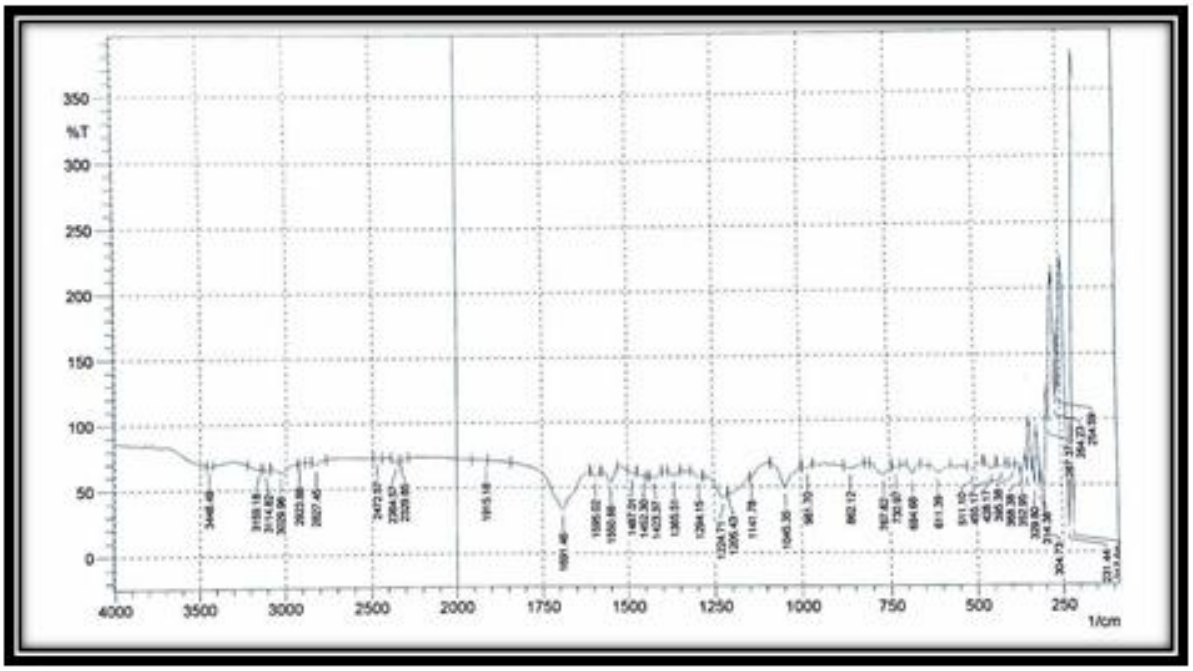

Figure (4): FTIR spectrum of $[Cu(SNT)_2Cl_2]$ Complex

Annals of R.S.C.B., ISSN:1583-6258, Vol. 25, Issue 4, 2021, Pages. 7968 - 8006
Received 05 March 2021; Accepted 01 April 2021.

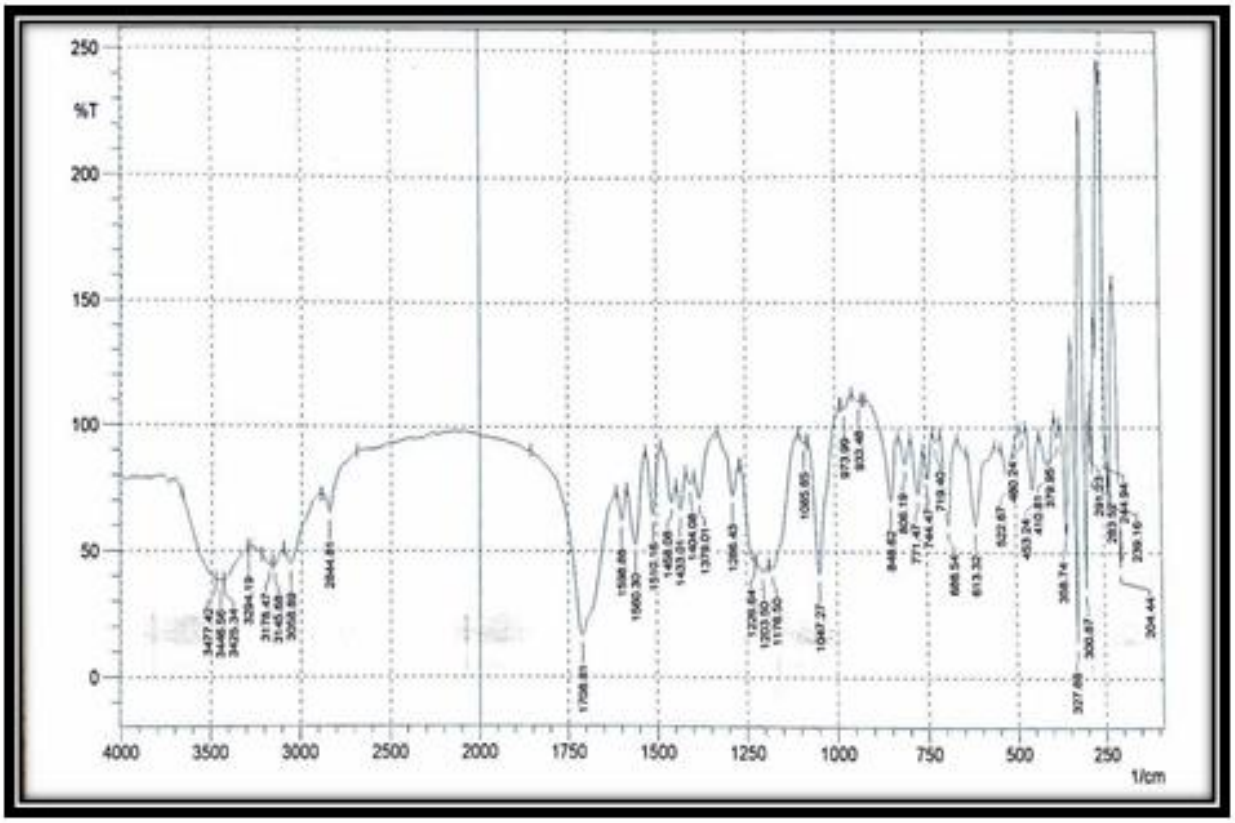

Figure (5): FTIR spectrum of$[Pt(SNT)_2Cl_2]$ Cl_2. H_2O complex.

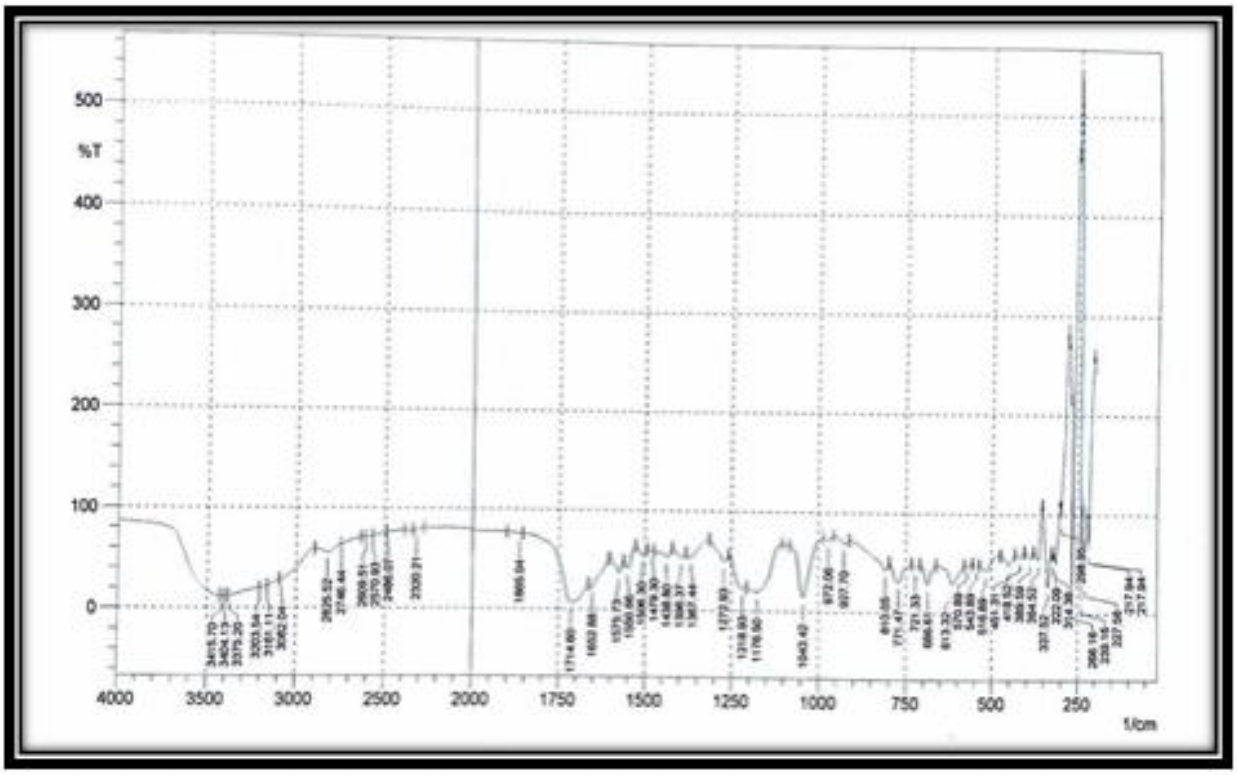

Figure (6): FTIR spectrum of $[Pd\ (SNT)_2]$ Cl_2 . H_2O complex

Annals of R.S.C.B., ISSN:1583-6258, Vol. 25, Issue 4, 2021, Pages. 7968 - 8006
Received 05 March 2021; Accepted 01 April 2021.

7-:1H-NMR

The ^{1}H-NMR studies are an additional support for the result obtained from the FT-IR spectra. Is achieved by considering the changes in the ^{1}H-NMR spectraof the synthesized complexes in comparison with the free ligand. The chemical shift data (δ) in ppm for different types of protons in the ligands (SNT) and their complexesforpd(II)andpt(IV)arereportedinTable(5)whiletheHNMRspectra were recorded in DMSO-d^{6} solution[Figure(7-9)].

The free ligand (SNT) display two singlet signals in the low field of TMS at (11.08and 8.71) ppm can be attributed to the protons of $(NH)_{prm}$ and (SO_3H) respectively [29]. The multiplet signals detected in the range (7.10-8.06) ppm are referred to the naphthyl and phenyl ring in the ligand (SNT)[30]

In the spectra of Pd (II) and Pt (IV) complexes all signals have a light change, reflecting the non-involvement of these groups in coordination with metal ion and also, supporting the involvement of $(N_{azo})$and (N_{imd}) in the coordination with Pd(II) and Pt(IV).

Table (5): ^{1}HNMR signals of SNT and their Complexes.

Compound	NH_{Pyim}	$COH_{ald.}$	SO_3H	$H_{arm.}$	$N\text{-}CH_{3\ Imd.}$	$N\text{-}CH_{3Pyrm}$	$Ar\text{-}CH_3$	H_2O
SNT	**11.08**	**-**	**8.71**	**7.48-7.39**	**3.87**	**3.37**	**-**	**-**
[Pd(SNT)$_2$] Cl$_2$ .H$_2$O	**11.08**	**-**	**8.82**	**8.30-7.86**	**3.81**	**3.47**	**-**	**3.34**
[Pt(SNT)$_2$Cl$_2$]Cl$_2$ .H$_2$O	**11.08**	**-**	**8.91**	**7.99-7.86**	**3.87**	**3.36**	**-**	**3.28**

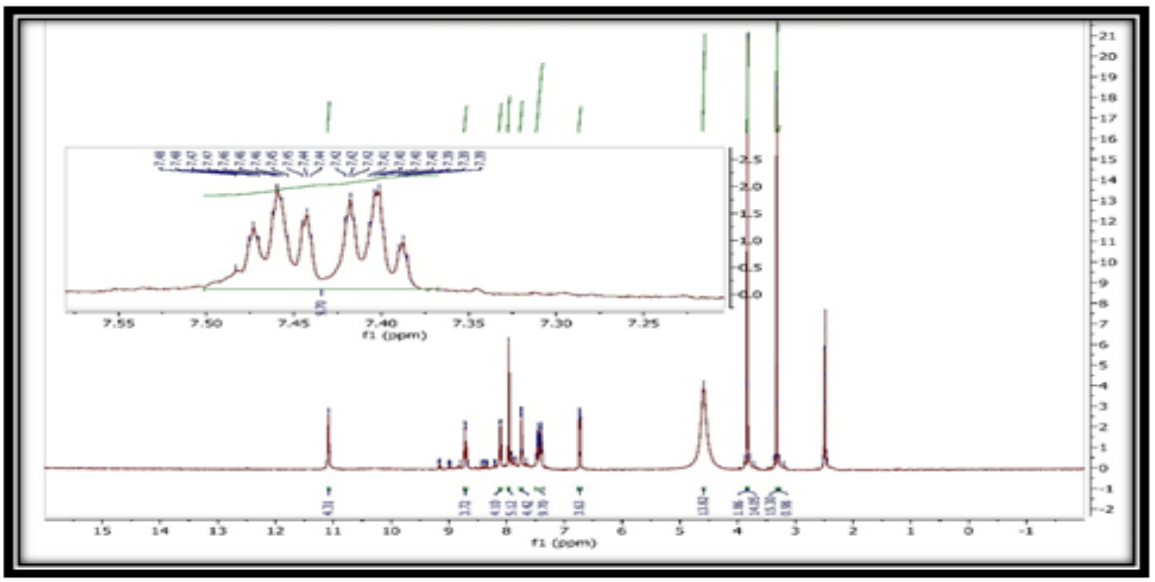

Figure(3 (7) INMR Spectrum for the SNT Ligand

Annals of R.S.C.B., ISSN:1583-6258, Vol. 25, Issue 4, 2021, Pages. 7968 - 8006
Received 05 March 2021; Accepted 01 April 2021.

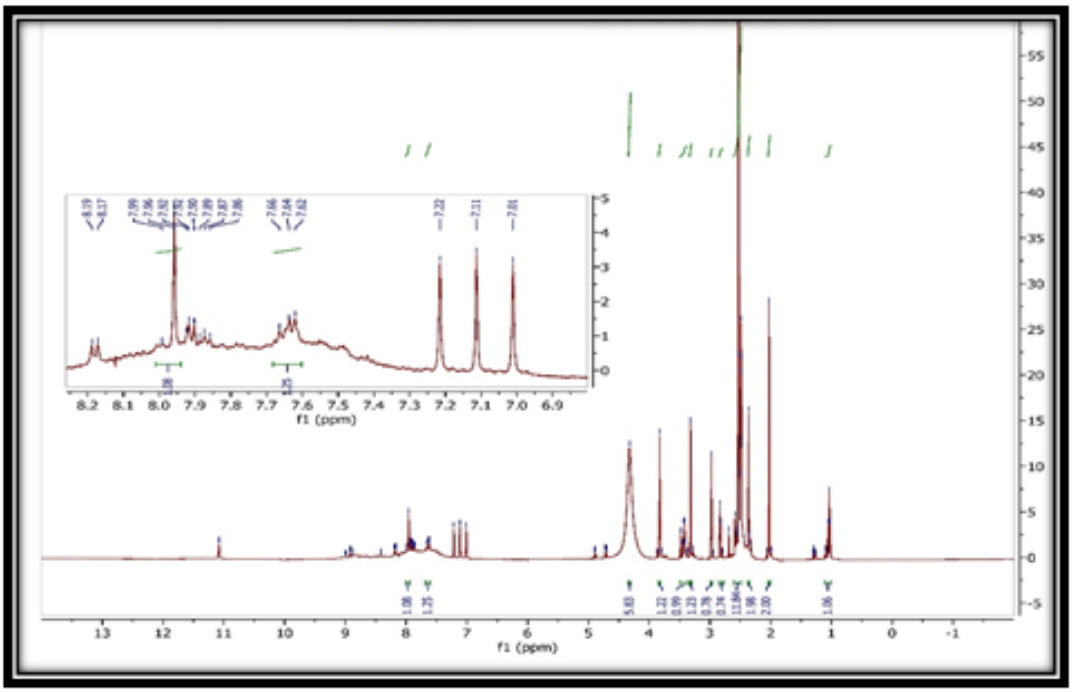

Figure(3-):^{1}HNMR Spectrum for the [Pt (SNT)$_2$Cl$_2$]Cl$_2$.H$_2$O complex.

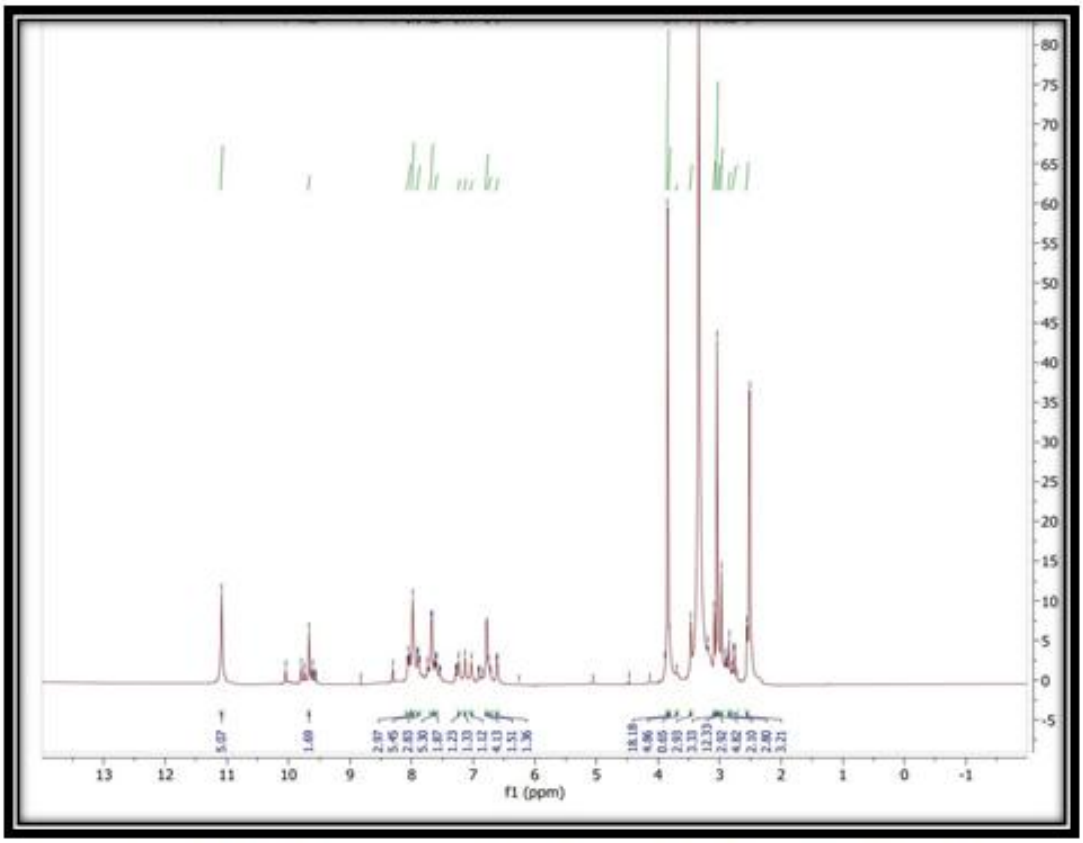

Figure(3-):^{1}HNMR Spectrum for the [Pd(SNT)$_2$]Cl$_2$.H$_2$O complex.

Annals of R.S.C.B., ISSN:1583-6258, Vol. 25, Issue 4, 2021, Pages. 7968 - 8006
Received 05 March 2021; Accepted 01 April 2021.

Magnetic properties and Electronicspectrum

The Electronic spectrum for the ligand (SNT) and its complexes were measured in ethanol (10^{-4}M) (against ethanol as reference) within the range (200-1100)nm.

The numerical date were listed in Table (6) and the electronic spectra were shown in Figures (10-14) .

The high bathochromic shift of λmax proposed the involvement of the ligand in the chelation with the metal ion [Ni(II), pd(II) , pt (IV)and Cu(II)] , while appeared in the area of low wave length the peaks due to(d-d) transition.

The ligand (SNT) displays mainly three peaks. The first and two peaks at (242nm,,41322m^{-1}) , (382nm ,26178cm^{-1}), were assigned to the moderate energy ($\pi - \pi$*) transition of the aromatic naphthalene and pyrimidine ring , while the third peaks at(512nm,19531cm^{-1}) was related to the n→ π* intermolecular transition charg transfer takingplace through the azo group and carbonyl group [31]

The spectrum of [Ni(SNT)$_2$ Cl$_2$]] complexes was shown three transitions Figure (11)

υ_1 =^{3}A$_2$g$_{(F)}$→^{3}T$_2$g $_{(F)}$ at (919nm,10881cm^{-1})and 892nm, 11210cm^{-1})

υ_2= ^{3}A$_2$g $_{(F)}$→^{3}T$_2$g $_{(F)}$ at (889nm,1124 cm^{-1})

υ_3= ^{3}A$_2$g $_{(F)}$→^{3}T$_2$g $_{(F)}$ at(520nm,19230cm^{-1})

These transition are characteristic for octahedral Ni(II) d^8 complex Moreover the magnitude of magnetic moment (2.9) B.M which consist with octahedral configuration high spin [32].

As for the band belonging to metal to ligand charge transfer (MLCT) nested with(υ_3).

In the spectrum of the low spin(d^8) pd(II) - complexes [Figers (12)], the peak was related to the ligand (SNT) which was shifted ,as expected to red shift by (14nm) The Three (d-d) transitions were predicted for square planar (d^8)^{1}A$_1$g → ^{1}A$_2$g,^{1}A$_1$g →^{1}B$_1$g and ^{1}A$_1$g →^{1}E$_1$g [33] Only two transtions were obseved at (916nm, 10917cm^{-1}),[(966nm,10905cm^{-1}) for pd(SNT)$_2$] Cl$_2$.H$_2$O which belonge to ^{1}A$_1$g^1 → ^{1}B$_1$g and ^{1}A$_1$g → ^{1}A$_2$g, receptively while the transitions ^{1}A$_1$g^1 → ^{1}E$_1$g may be hiddin by the (M LCT) band at (556nm,17985cm^{-1}) for so the magnetic moment is zero and diamagnetic .

The electronic spectrum of high spin pt (IV) complex was showed a red shift of the $\pi \rightarrow \pi$* transition for the ligand SNT from (512nm,cm^{-1}) to(666nm , cm^{-1}) as was shown in Figure (13) There are three (d-d) transitions were expected for Pt(IV) -complexes (d^6), octahedral with diamagnetic properties in the visible region [34]

^{3}A$_2$g→^{1}T$_1$g

^{3}A$_2$g→^{1}T$_2$g

^{3}A$_2$g→^{3}T$_3$g(forbiden transition)

All transition were included in Table (6) for the synthesized pt(IV) –complex with diamagnetic properties.

Finally The magnetic moment value of the synthesized Cu(II) – complex (1.86B.M) lie within the range of Cu (II)d^9 (ion The electronic spectrum of [Cu (SNT)$_2$Cl$_2$] appeared abroad band at (616m,16233cm^{-1}) which related to ^{2}B$_1$g →^{2}Eg and ^{2}B$_1$g →^{2}B$_2$g, in a tetragonally distorted octahedral (D$_4$h) [35].

Annals of R.S.C.B., ISSN:1583-6258, Vol. 25, Issue 4, 2021, Pages. 7968 - 8006
Received 05 March 2021; Accepted 01 April 2021.

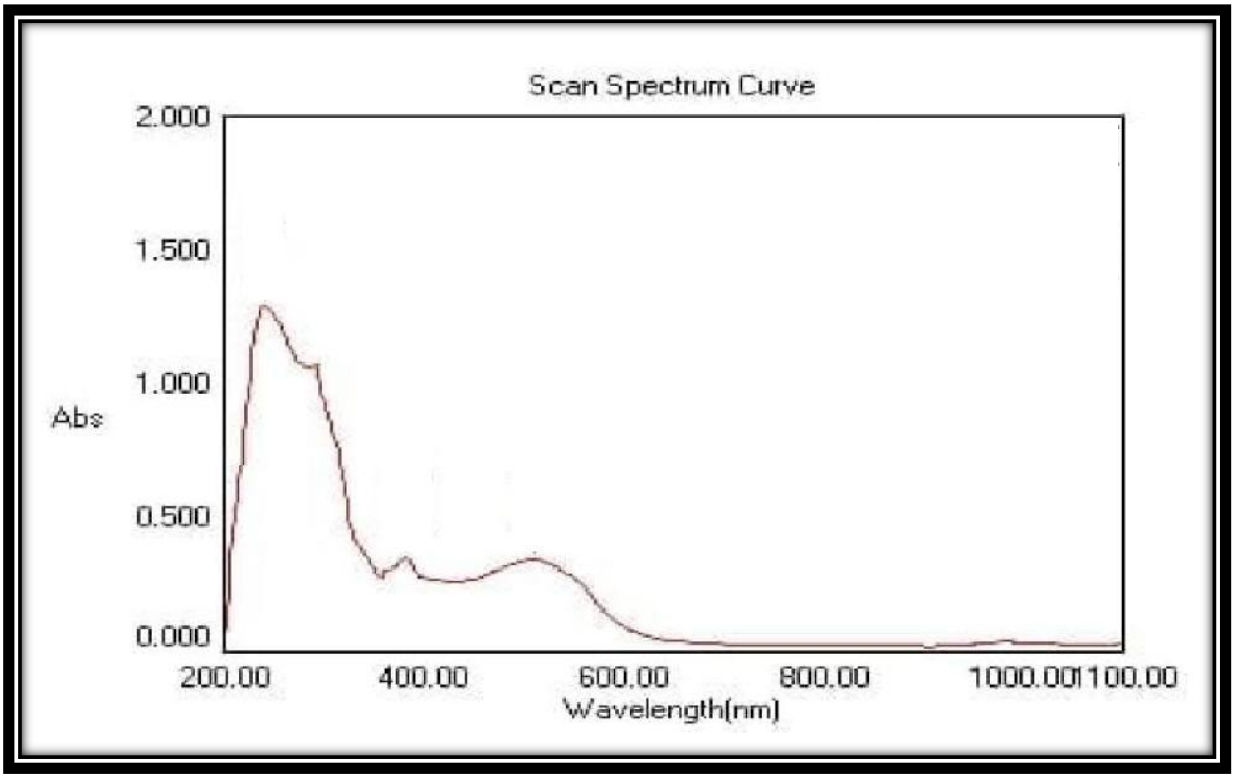

Fig.(10) : UV-Vis Spectrum for the SNT.

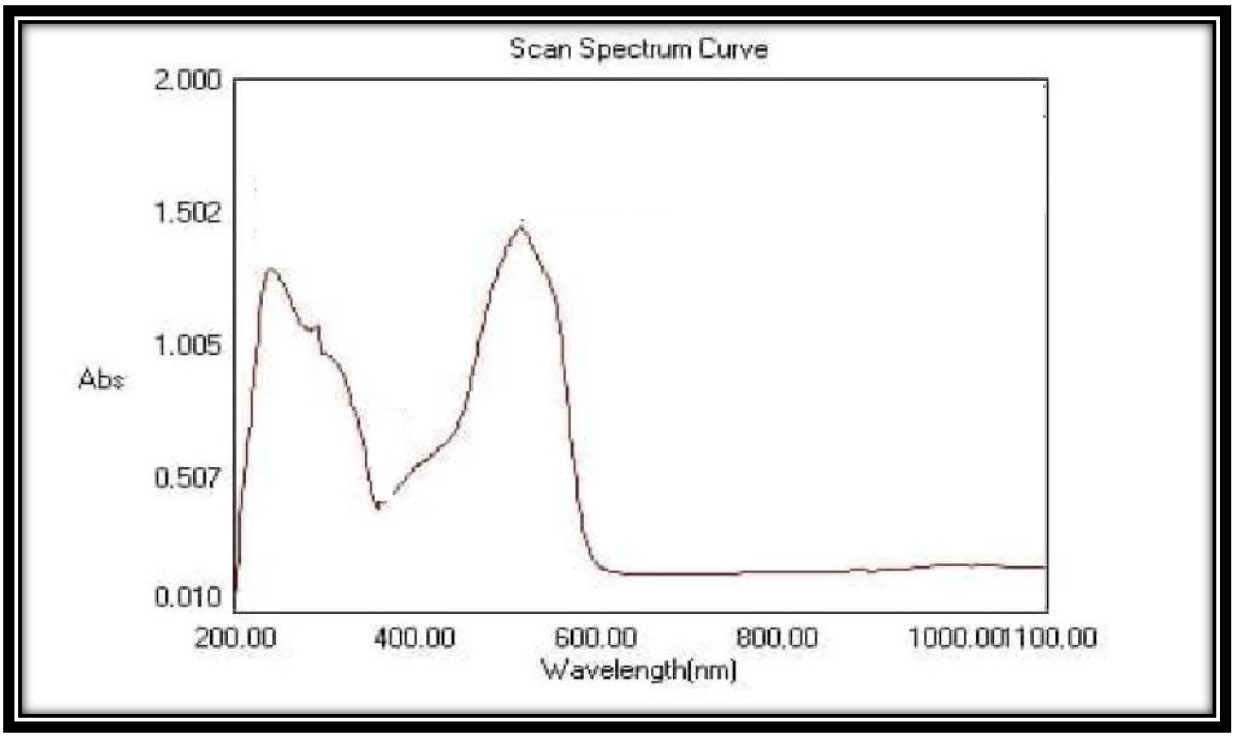

Fig. (11) : UV-Vis Spectrum for the Ni(II)-SNT.

Annals of R.S.C.B., ISSN:1583-6258, Vol. 25, Issue 4, 2021, Pages. 7968 - 8006
Received 05 March 2021; Accepted 01 April 2021.

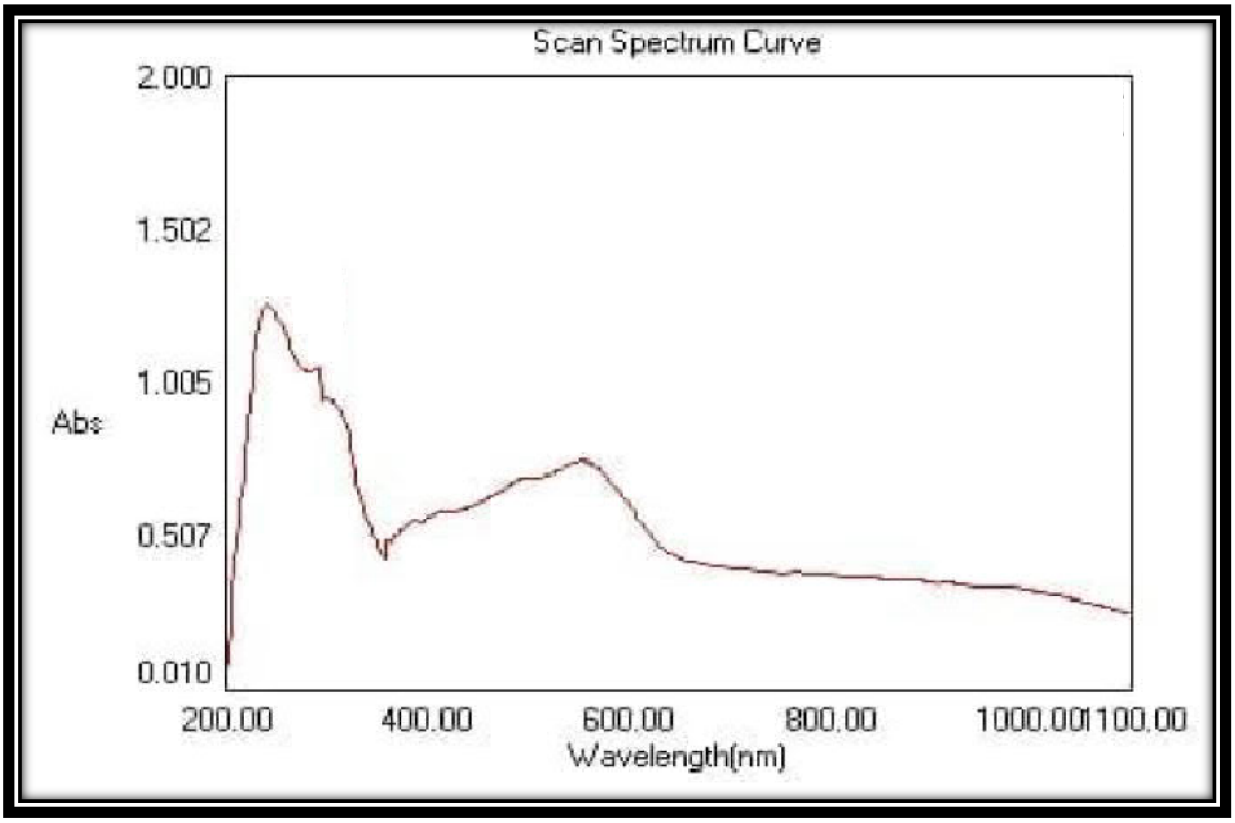

Fig.(12): UV-Vis Spectrum for the Pd(II)-SNT.

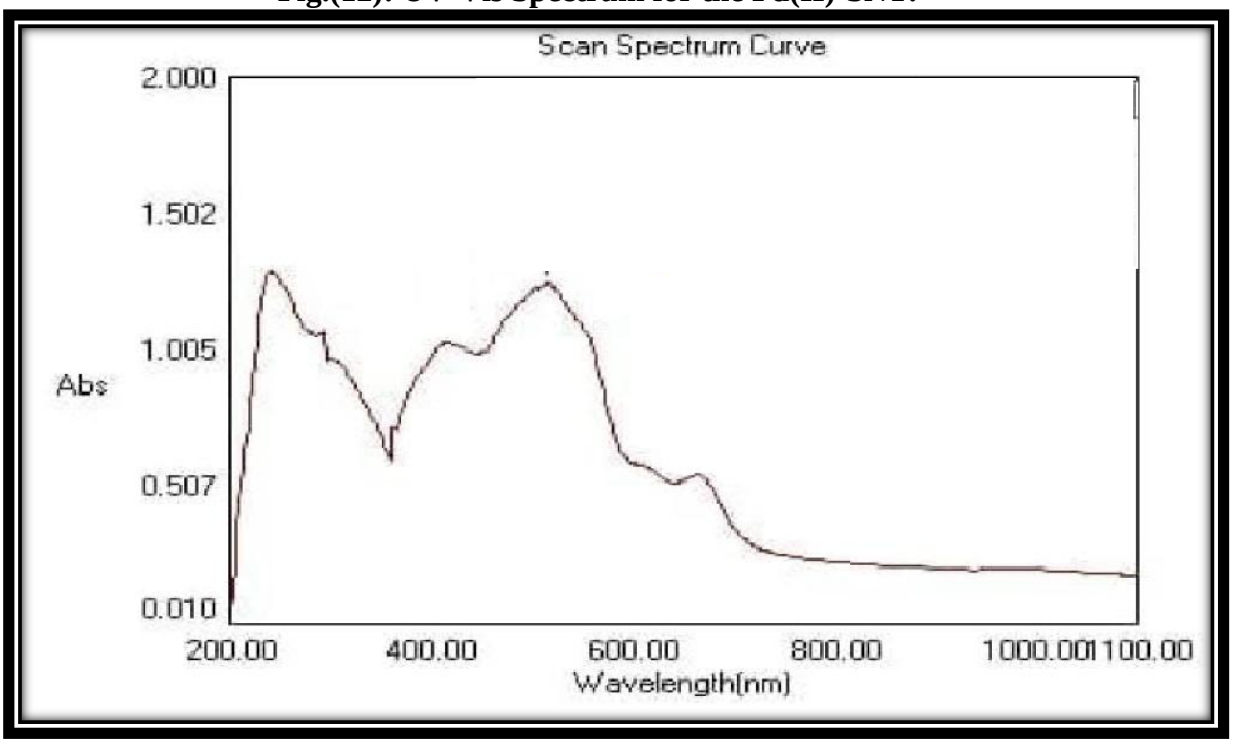

Fig.(13): UV-Vis Spectrum for the Pt(IV)-SNT.

Annals of R.S.C.B., ISSN:1583-6258, Vol. 25, Issue 4, 2021, Pages. 7968 - 8006
Received 05 March 2021; Accepted 01 April 2021.

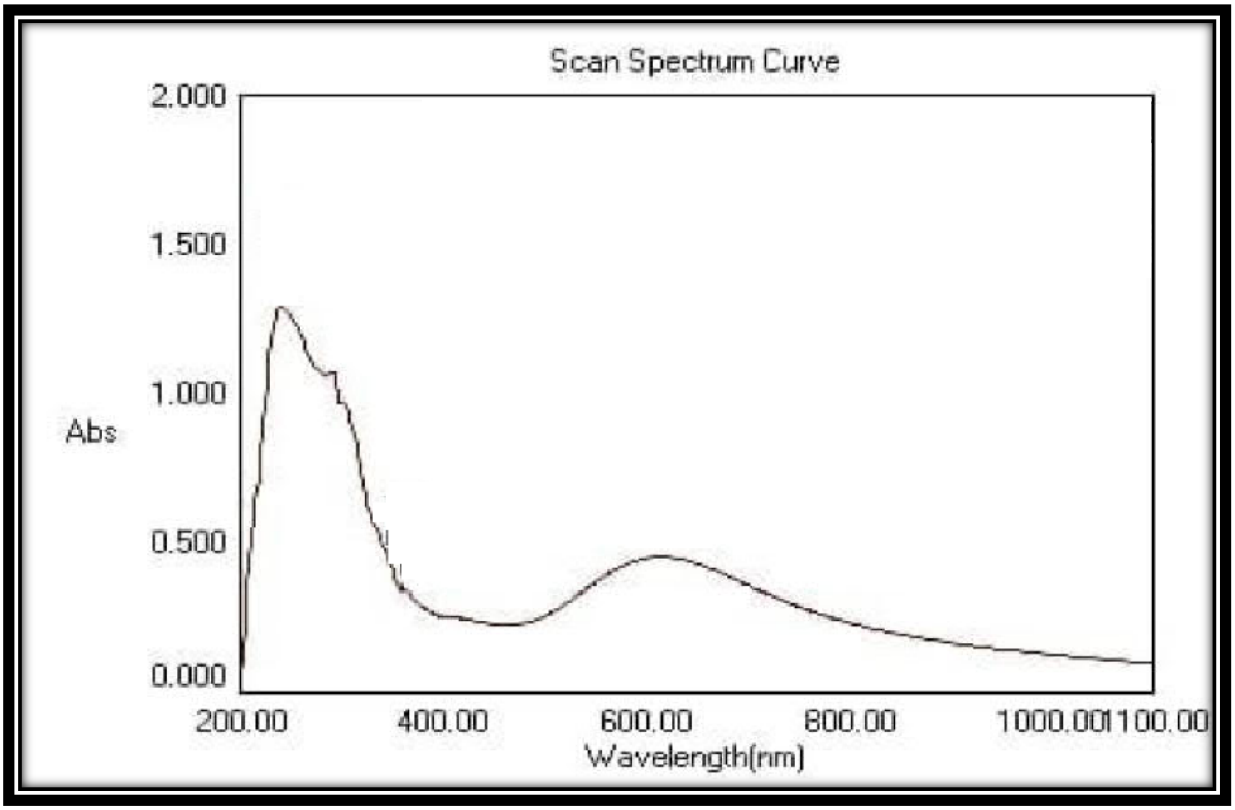

Fig. (14) : UV-Vis Spectrum for the Cu (II) - SNT .

Table(6): Electronic transition, hybridization and geometry at the ligand and their complex's at (10^{-4}M)

Compound	λ	Wavenumber (cm^{-1})	Assignment	hybridization	Geometry
SNT	242 362 512	41322 27624 19531	$\pi \rightarrow \pi^*$ $n \rightarrow \pi^*$ $\pi \rightarrow \pi^*$	_____	_____
$[Ni(SNT)_2Cl_2]$	242 366 520 889 919	41322 27322 19230 11248 10881	$\pi \rightarrow \pi^*$ $n \rightarrow \pi^*$ $^3A_2g_{(F)} \rightarrow {}^3T_2g_{(p)}$ $^3A_2g_{(F)} \rightarrow {}^3T_2g_{(F)}$ $^3A_2g_{(F)} \rightarrow T_1g_{(F)}$	Sp^3d^2	octahedral
$[Pd(SNT)_2]$ $Cl_2.H_2O$	298 556 916 966	33557 17985 10917 10351	$\pi \rightarrow \pi^*$ MLCT $^1B_1g \rightarrow {}^1A_1g$ $^1A_1g \rightarrow {}^1T_2g$	Sp^3d	Square planer
$[Pt(SNT)_2d_2]$ $Cl_2.H_2O$	242 416 516 666 917 976	41332 24038 19379 15015 10905 10245	$\pi \rightarrow \pi^*$ $n \rightarrow \pi^*$ MLCT $^1A_1g \rightarrow {}^1T_1g$ $^1A_1g \rightarrow {}^1T_2g$ $^1A_1g \rightarrow {}^3T_1g$	$d^2\ Sp^3$	octahedral
$[Cu(SNT)_2Cl_2]$	242 362 616	41322 27624 16233	$\pi \rightarrow \pi^*$ $n \rightarrow \pi^*$ $^2B_1g \rightarrow {}^2Eg_+ {}^2B_1g \rightarrow {}^2B_2g$	Sp^3d^2	Tetragonal

Annals of R.S.C.B., ISSN:1583-6258, Vol. 25, Issue 4, 2021, Pages. 7968 - 8006
Received 05 March 2021; Accepted 01 April 2021.

8-Thermo gravimetric Analysis (TGA) and Differential scanning colorimetry (DSC)

The Thermo gravimetric analysis has a major role in assessing the properties for the compounds aside from stoichiometry for the dented volatile decomposition products. The investigated ligand (SNT) and its complexes were suspected, in argon flow within the temperature range (25 – 1000) C^o The number of stages, stages of degradation, the calculated and the obtained weight loss percentages, degradation product loss and the residues are listed in Table (7) and represented graphically in Figures [(15-19)]

The results were showed that the ligand and its complexes were decomposed in (3-5) steps with exothermic effect in DSC curve . The hydrated water molecule were volatilize within temperature rang (25-200)C^o, . All complexes were displayed the decomposition of the organic ligand within the range (200 – 1000) C^o leading to metal oxid as residue. As well As from Table (7) we conclude the following :

1- The thermal stability of the new compounds are :
[pd $(SNT)_2$] Cl_2 .H_2O>*SNT*>[*Pt*$(SNT)_2$] Cl_2 .H_2O>[Cu $(SNT)_2$ Cl_2]> Ni $(SNT)_2$ Cl_2
2- The results are showed in good agreement with the formula suggested from analytical results .

Table (7): (TGA) and (DSC) of ligand (SNT) and its complexes

Com. Sym.	Molecular formula(molecular weight) g/mole	Step	TG. Range of the decomposition (°C)	Suggested Assignment	Mass loss %		DSC °C
					Calculate %	Found %	
SNT	C17H14N6O5S) (414.404)	1	25-230 C^o	Hcl C_2 H_2	6.48	6.50	230.59 EXO
		2	230-575 C^o	C_{32} H_{25} CL N_{12} S2 O_4	76.89	77.07	318.38 EXO
		3	575-1000 C^o		15.90	15.70	
		Residue			0.65	<1000 C^o	
[Ni(SNT)$_2$Cl$_2$]	NiC34H28N12O10S2Cl2 (958.498)	1	25-455 C^o	C34H28N12Cl2S2O7	88.78	89.02	345.72 EXO
		2	455-1000 C^o	Ni0.89O3	10.45	10.3	
		3					
		Residue		0.11Ni	0.67	0.68	
[Cu(SNT)$_2$Cl$_2$]	CuC34H30N12O11S2Cl2 (963.348)	1	25-230 C^o	C5H3	6.54	6.5	208.77 EXO
		2	230-565 C^o	C29H25Cl2N12S2O45	77.72	77.07	331.34 EXO
		3	565-1000 C^o	0.88CuO6.5	16.61	15.70	619.70 EXO
		Residue		0.12Cu	0.79	0.73	
[Pd(SNT)2]Cl2 .H2O	PdC34H30N12O11S2Cl	1	25-160 C^o	$H_{14}O$	2.92	2.82	95.93 EXO
		2	160-490 C^o	C_{34} H_6 Cl_2 N_5	54.18	54.26	327.9

Annals of R.S.C.B., ISSN:1583-6258, Vol. 25, Issue 4, 2021, Pages. 7968 - 8006
Received 05 March 2021; Accepted 01 April 2021.

	4 (1024.228)						3 EXO
		3	490-1000 C^o	H_{10} N_6 S_2	15.42	15.71	
		Residue		Pd O_{10} N	27.37	27.21	
[Pt(SNT)$_2$Cl$_2$]Cl$_2$ .H$_2$O	PtC34H30N12O11S2Cl4 (1083.892)	1	25-125 C^o	H_9O	2.11	2.14	
		2	125-400 C^o	C_{34} H_{21} Cl_4	48.23	48.39	333.63 EXO
		3	400-570 C^o	N_5 S_2	11.31	11.05	431.32 EXO
		4	570-750 C^o	N_6	7.09	7.01	681.14 EXO
		5	750-1000 C^o	NO_7	10.64	10.67	812.65 EXO
		Residue	>1000 C^o	PtO_4	21.81	20.73	

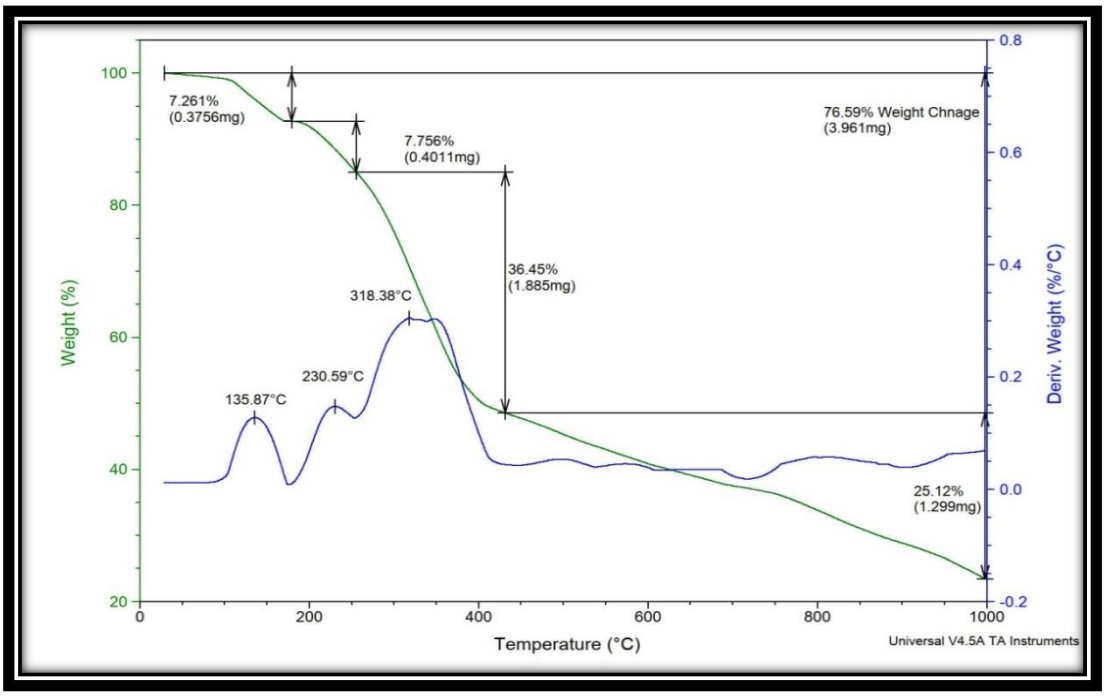

Figure (15): DSC-TGA for the (SNT) of the ligand

Annals of R.S.C.B., ISSN:1583-6258, Vol. 25, Issue 4, 2021, Pages. 7968 - 8006
Received 05 March 2021; Accepted 01 April 2021.

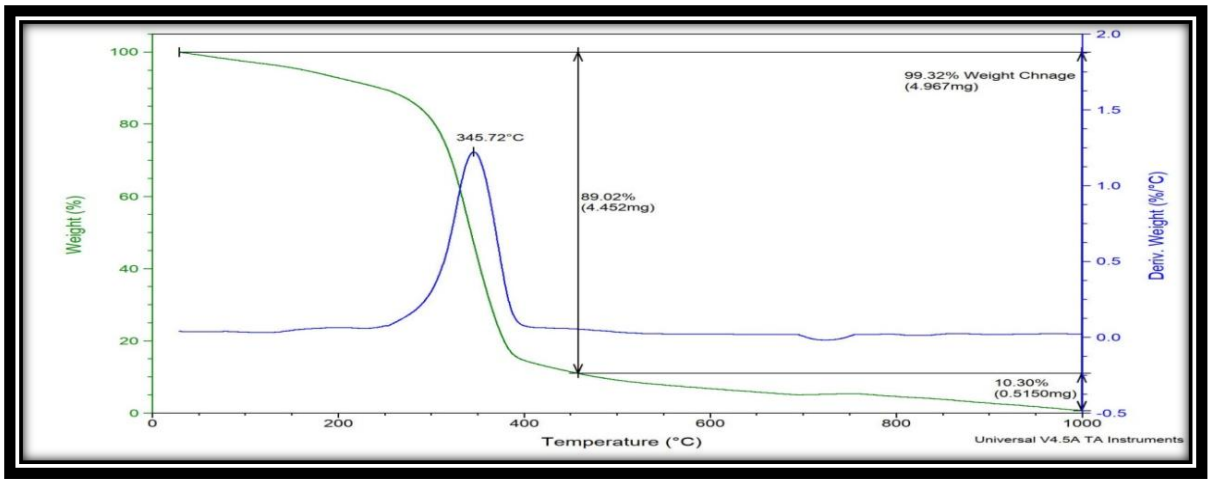

Figure (16): DSC-TGA for the [Ni(SNT)$_2$Cl$_2$] Complex

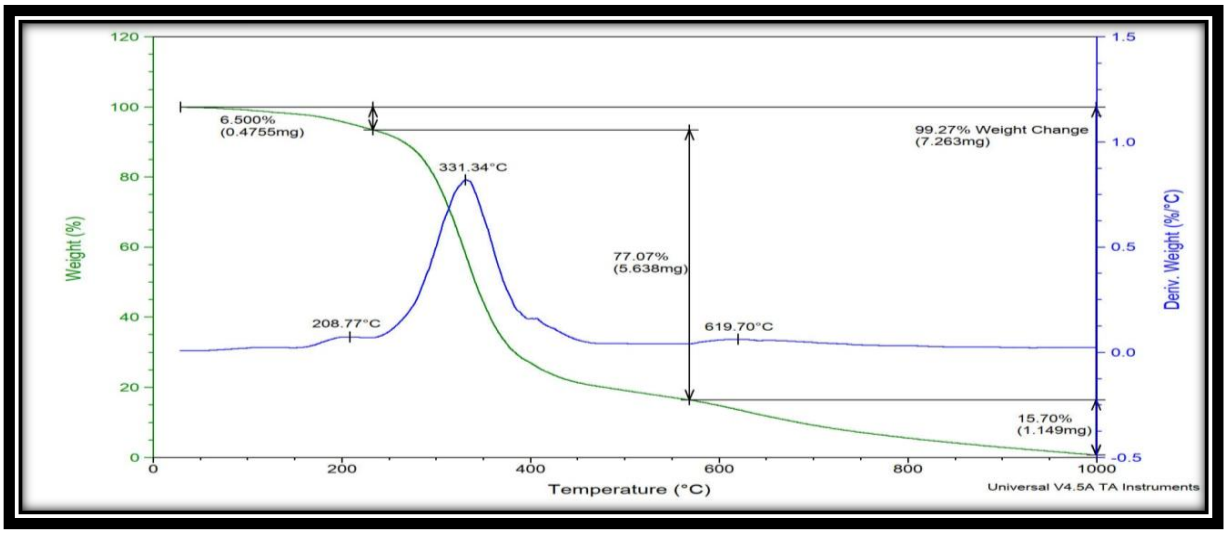

Figure (17): DSC-TGA for the [Cu(SNT)$_2$Cl$_2$] Complex

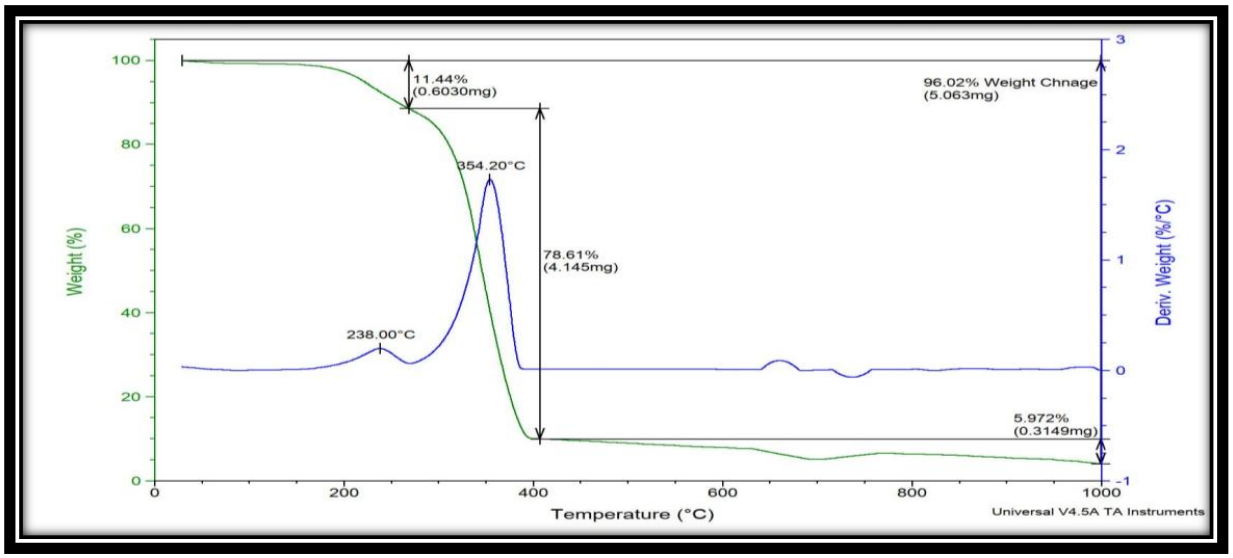

Figure (18): DSC-TGA for the [Pd (SNT)$_2$] Cl$_2$ .H$_2$O Complex

Annals of R.S.C.B., ISSN:1583-6258, Vol. 25, Issue 4, 2021, Pages. 7968 - 8006
Received 05 March 2021; Accepted 01 April 2021.

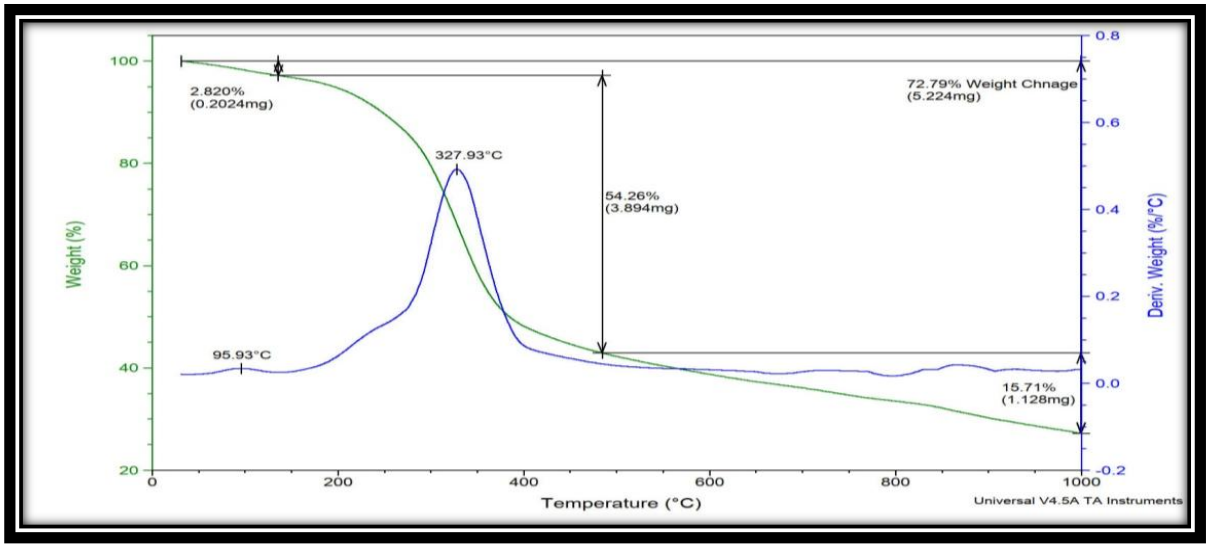

Figure (19): DSC-TGA for the $[Pt(SNT)_2Cl_2]Cl_2.H_2O$ Complex

9-Scanning Electron microscopy Analysis (SEM)

the topographical surface of different samples shows the micro structures of these surfaces . the electrons were interested with the atoms in the sample , producing various signds that contain information about the topography and composition of the surface [36]

The morphology for the ligand (SNT) with their complexes was appeared different crystal line structures and surface homogeneities. An accreditation was done in SEM technique on area of a cross section (100nm) and enlarging power (Mag=60.00KX) as was shown in Figure [(20-24)]. The SEM images explained heterogeneous surfaces with different shapes soit varies with different compound and difference volume for paricale [Table](11).

Table(11).SEM date for the ligand(SNT) and its complexes

Compound	Average volume (nm)	shape
SNT	231.64	Cubic
$[Ni(SNT)_2Cl_2]$	100.56	Coral
$[Pd(SNT)_2]\ Cl_2.H_2O$	348.24	Different shape
$[Pt(SNT)_2d_2]\ Cl_2.H_2O$	170.06	Different shape
$[Cu(SNT)_2Cl_2]$	103.11	Spherical

Annals of R.S.C.B., ISSN:1583-6258, Vol. 25, Issue 4, 2021, Pages. 7968 - 8006
Received 05 March 2021; Accepted 01 April 2021.

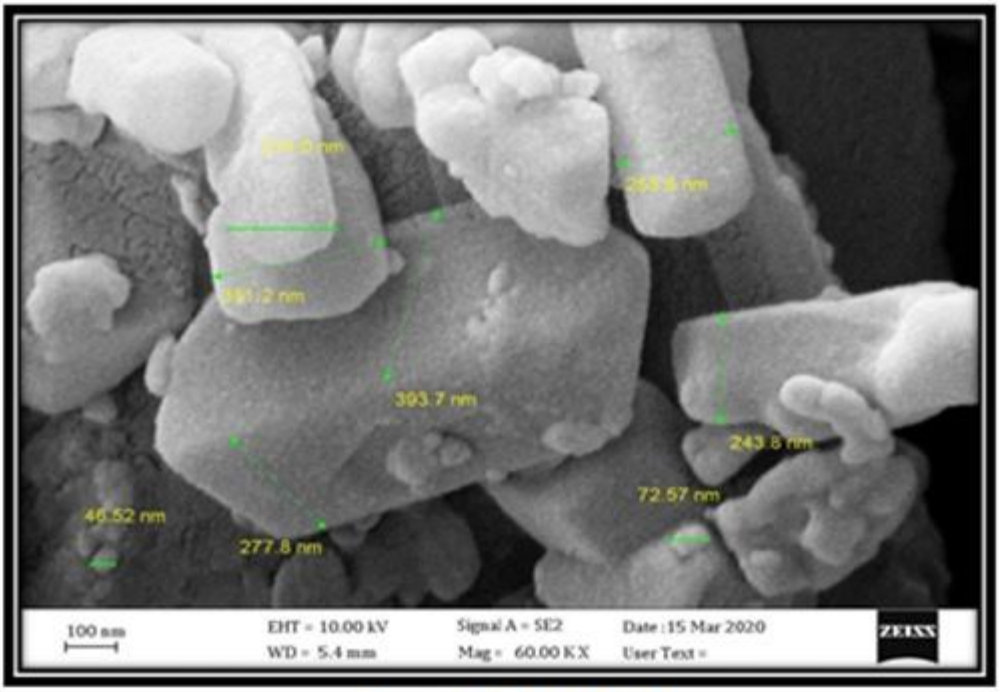

Figure (21) [SNT]

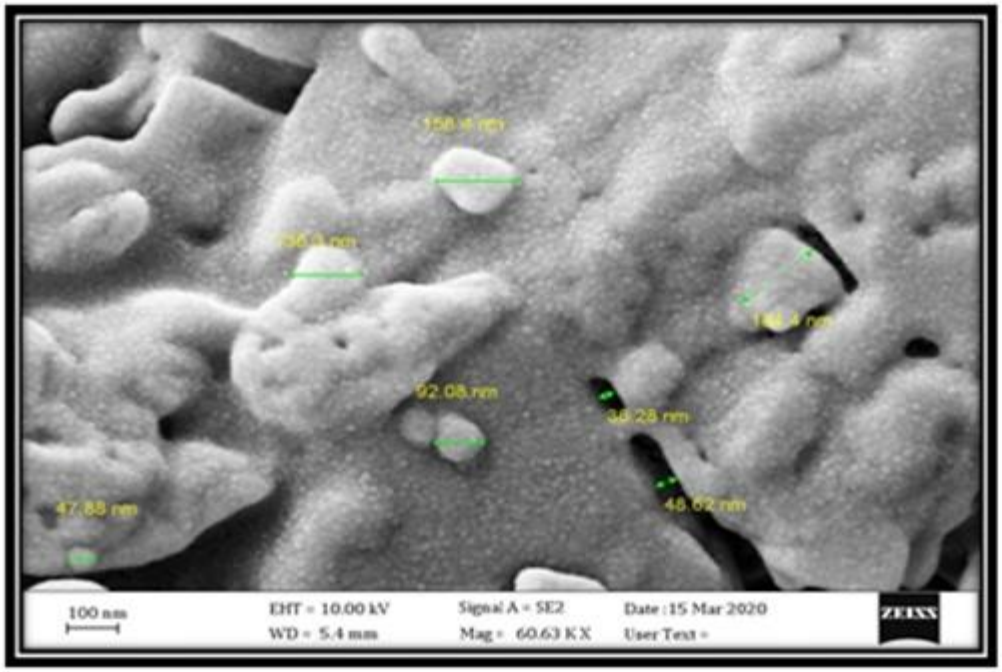

Figure (22) $[Ni(SNT)_2Cl_2]$

Annals of R.S.C.B., ISSN:1583-6258, Vol. 25, Issue 4, 2021, Pages. 7968 - 8006
Received 05 March 2021; Accepted 01 April 2021.

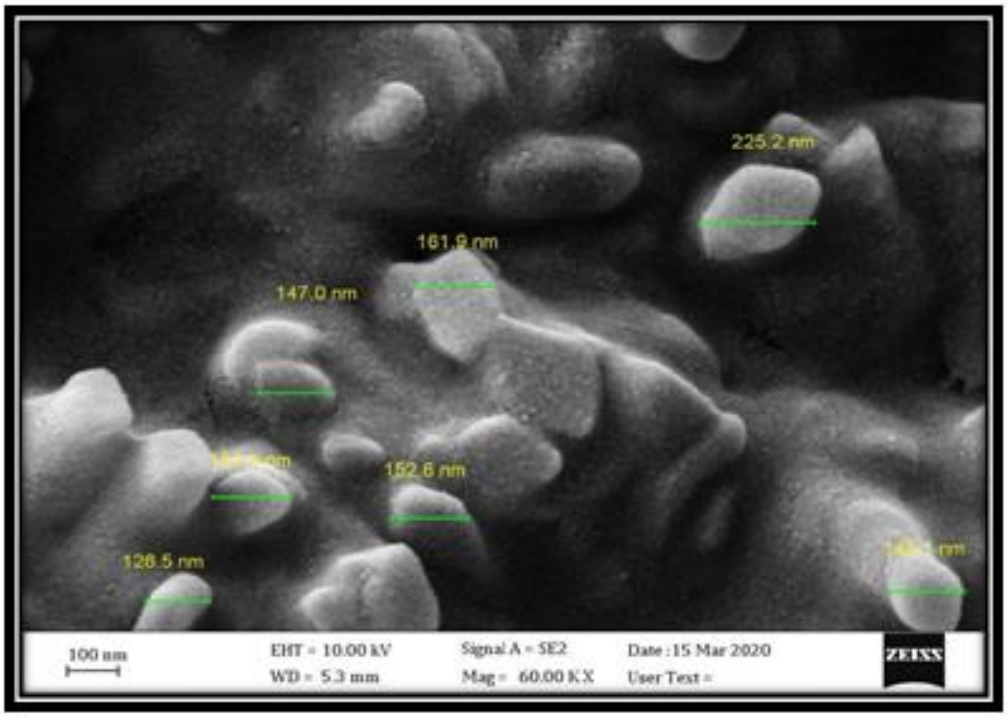

Figure (22) SEM for $[Cu(SNT)_2cl_2]$

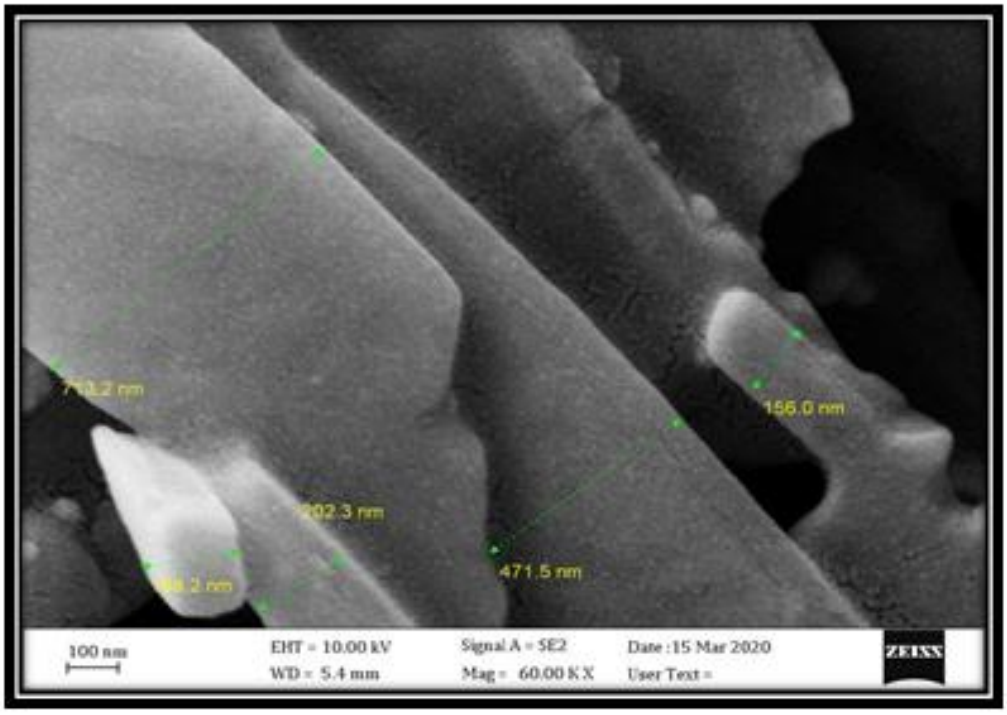

Figure (24) $[Pd(SNT)_2]\ Cl_2.H_2O$

Annals of R.S.C.B., ISSN:1583-6258, Vol. 25, Issue 4, 2021, Pages. 7968 - 8006
Received 05 March 2021; Accepted 01 April 2021.

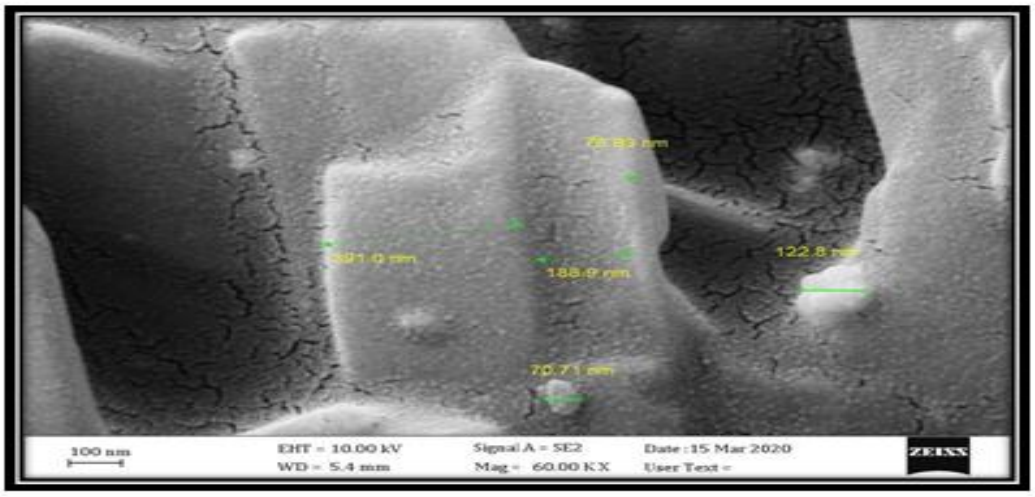

Figure (25) $[Pt(SNT)_2d_2]$ $Cl_2.H_2O$

10-Antibactiralof the SNTand their metal complexes

supervision of microbial population is important to prohibit show of infection, disease, damage and contamination caused by them. The novel azo ligand (SNT) and its complexes were screened for antimicrobial efficiency in vitro with four pathogenic microorganisms by disk diffusion process [37]. The microorganisms utilized were of Pathogenic nature and have been specified to cause much life –threatening diseases in living system. They were two gram –negative bacteria species (*E.coli and Klebsiella*) and to gram-positive bacteria species (*Streptococcus and Staphylococcus*). All obtained results are reported in Table (9) and represented in Figure (25). From the results obtained, all of the tested compounds have moderate to strong efficiency except nickel (II)complexes , has been showed no efficiency with all type of selected bacteria their where compared withAmoxicillin as a reference antibacterial and appeared good inhibition to the same pathogenic bacteria .Through the obtained result, its concluded that the synthesized compounds may be integrated into DNA helix chains in bacteria molecules , which are available to damage theMicroorganism's biological methods . On the other hand the coordination bonds between the azo ligand (SNT) and selected metal ions may enhance the efficiency with various bacteria species due to the overtone concept of cell permeability protein that the cell is enclosed with a lipid membrane, which favors the passing only lipid soluble materials[38] . In coordination the positive charge of metal ion is partially shared with ligand donor atom, and thus there is electron delocalization over the whole coordination ring. So , the lipophilicity of the compounds are increased . The penetration of the metal ions complexes in to lipid membrane will increase, which owing to blocking of the metal binding sites on enzymes for microorganisms. Moreover, the formation of bacterial cell wall be ruptured, they will perish and the growth of the organism will be stop. Finally, these compounds also destroy the respiration process of the cell, which leads to not synthesis of proteins [39].

Table (12): The inhibition zones scale in (mm) of Amoxicillin, ligand (SNT) and its complexes

Compounds.000000	**Gram Negative**		**Gram Positive**	
	Escherichia coli	***klebsiella***	***streptococcus***	***Staphylococcus***

Annals of R.S.C.B., ISSN:1583-6258, Vol. 25, Issue 4, 2021, Pages. 7968 - 8006
Received 05 March 2021; Accepted 01 April 2021.

Amoxicillin		15	10	12	14
1	**SNT**	10	10	10	10
2	**$[Ni(SNT)_2Cl_2]$**	0	0	0	0
3	**$[Cu(SNT)_2Cl_2]$**	0	10	0	0
4	**$[Pd(SNT)_2]Cl_2 .H_2O$**	10	15	16	15
5	**$[Pt(SNT)_2Cl_2]Cl_2.H_2O$**	10	0	10	10

(E-Coli)

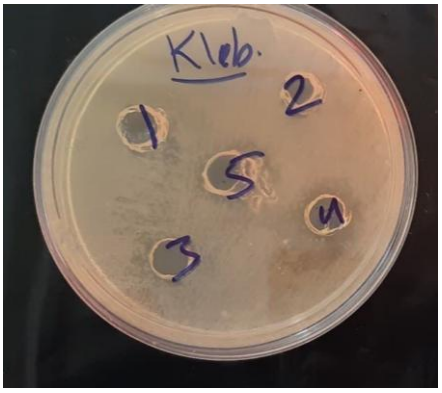

(klebsiella)

(Streptococc)

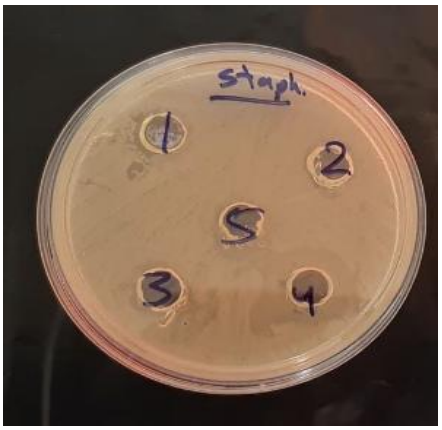

(Staphylococcus

Figure (25): The inhibition zone for SNT and its complexes

11-The Cytotoxic Effecrs

Since the find out of cisplatin , many new pt and pdcomplexes have been synthesized and estimated for their cytotoxic activity Although there are different drugs for the treating carcinoma, still it remains the main cause of death worldwide because of limitations such as multidrug resistance.high toxicity and adverse side effects [40] therefore, they have been many defrosts to find compounds which is might serve as more effective less toxic and adverse side effects anticaranoma drugs [41].Thus , recent studies have been converged on the synthesizing of effective compounds having heterocyclic ring aschemotherapeutic drugs [42]. And well to define the performance of any now compound that can be utilized as anticaranoma drugs it is necessary to define how it improves clinical land hematological

Annals of R.S.C.B., ISSN:1583-6258, Vol. 25, Issue 4, 2021, Pages. 7968 - 8006
Received 05 March 2021; Accepted 01 April 2021.

fastors, the biochemical profile and reduces fertile tumor call counting in the host and also prolongs the life span [43].

In this divection, we have investigated the cytotoxic activity and mechanism of action for the synthesized (SNT) ligand with its[$(Pd(II))$and pt(III)] complexes against lung carcinoma cell line (A549) and normal cell line (WRL68) by MTT assay after incubated for 24hr and 72hr at 37C° and with concentrations (10,20,30,50,100) μg/ml.It was found that the selected compounds had various growth inhibitory effects on A549 and WRL68 cell line the extetent at toxic effect was estimated by measuring the percentage of cell growth inhibition compared to the control. the results from Table $[(13-15)]$ andFigures (26-28) .were shown that, after incubation at concentration (10-100) μg /ml of the(SNT), and selected complexes for 24 hrs and 72 hrs with A549 and WRL68 cells line ,a series of morphological modifications for DNA inclusive condensation fragmentation of chromatin and nucleus with formation of opoptotic bodies were observed which was the proof of apoptosis and drug potential of the tested compound [44].

Table (13) Evolution at cytotoxicity of the ligand (SNT) against A549 censer cell line and WRL – 68 cell line after incubation for (24 hours) at (37)℃

Cell line	Concentration (Mg/ml)					Number of values	IC 50 Mg/ml	p-value
	10	20	30	50	100			
A_{549}	95.062 ∓ 1.341	94.560 ∓ 0.759	94.637 ∓1.802	81.983 ∓ 0.372	70.988 ∓ 1.275	3	49.22	<0.0001
WRL-68	94.599 ∓ 0.291	94.599 ∓ 0.735	93.982 ∓ 2.729	86.729 ∓ 1.205	76.968 ∓ 1.446	3	52.12	

After incubation for (72 hours) at (37)℃

Cell line	Concentration (Mg/ml)					Number of values	IC 50 Mg/ml	p-value
	10	20	30	50	100			
A_{549}	95.949 ∓ 0.909	83.457 ∓2.039	61.381 ∓ 1.275	52.122 ∓ 3.848	39.429 ∓ 2.793	3	26.50	<0.0001
WRL-68	82.986 ∓ 0.504	83.873 ∓ 1.718	79.707 ∓ 1.753	73.611 ∓ 2.523	59.221 ∓0.965	3	65.4	

Annals of R.S.C.B., ISSN:1583-6258, Vol. 25, Issue 4, 2021, Pages. 7968 - 8006
Received 05 March 2021· Accepted 01 April 2021

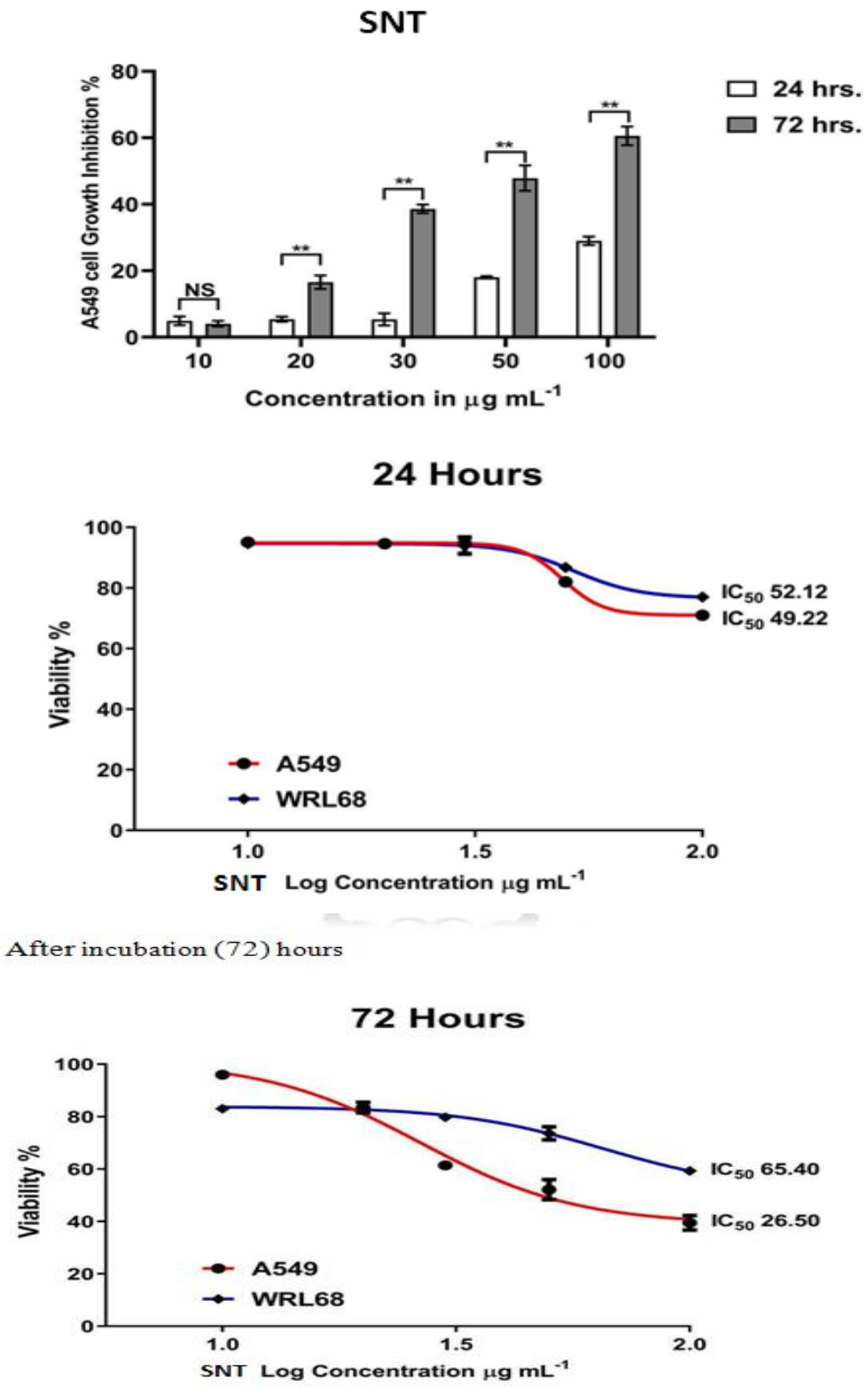

Figure (26)cytotoxicity effect of (SNT)on A_{549} cancer cell line and WRL-68 cell line after incubation (24and72hours)

Annals of R.S.C.B., ISSN:1583-6258, Vol. 25, Issue 4, 2021, Pages. 7968 - 8006
Received 05 March 2021; Accepted 01 April 2021.

Table (14) Evaluation of cytotoxicity of $[pt(SNT)_2Cl_2]Cl_2.H_2O$ against A_{549} cancer cell line after incubation (24 hours) at ($37C^o$) and WRL-68 cell line

Cell line	Concentration (Mg/ml)					Number of values	IC 50 Mg/ml	p-value
	10	20	30	50	100			
A_{549}	94.792 ∓ 1.335	88.272 ∓ 2.568	75.309 ∓ 4.148	63.696 ∓ 2.123	59.915 ∓ 3.323	3	28.2	<0.001
WRL-68	96.952 ∓ 1.142	96.180 ∓1.252	87.114 ∓ 3.649	74.460 ∓ 0.854	65.702 ∓ .654	3	38.17	

After incubation (72 hours) at ($37C^o$)

Cell line	Concentration (Mg/ml)					Number of values	IC 50 Mg/ml	p-value
	10	20	30	50	100			
A_{549}	84.144 ∓ 0.810	71.026 ∓ 1.075	59.529 ∓ 1.226	49.961 ∓2.135	49.383 ∓3.021	3	22.62	<0.001
WRL-68	83.642 ∓0.821	82.986 ∓ 1.422	74.306 ∓ 5.171	63.195 ∓2.652	51.119 ∓2.100	3	43.14	

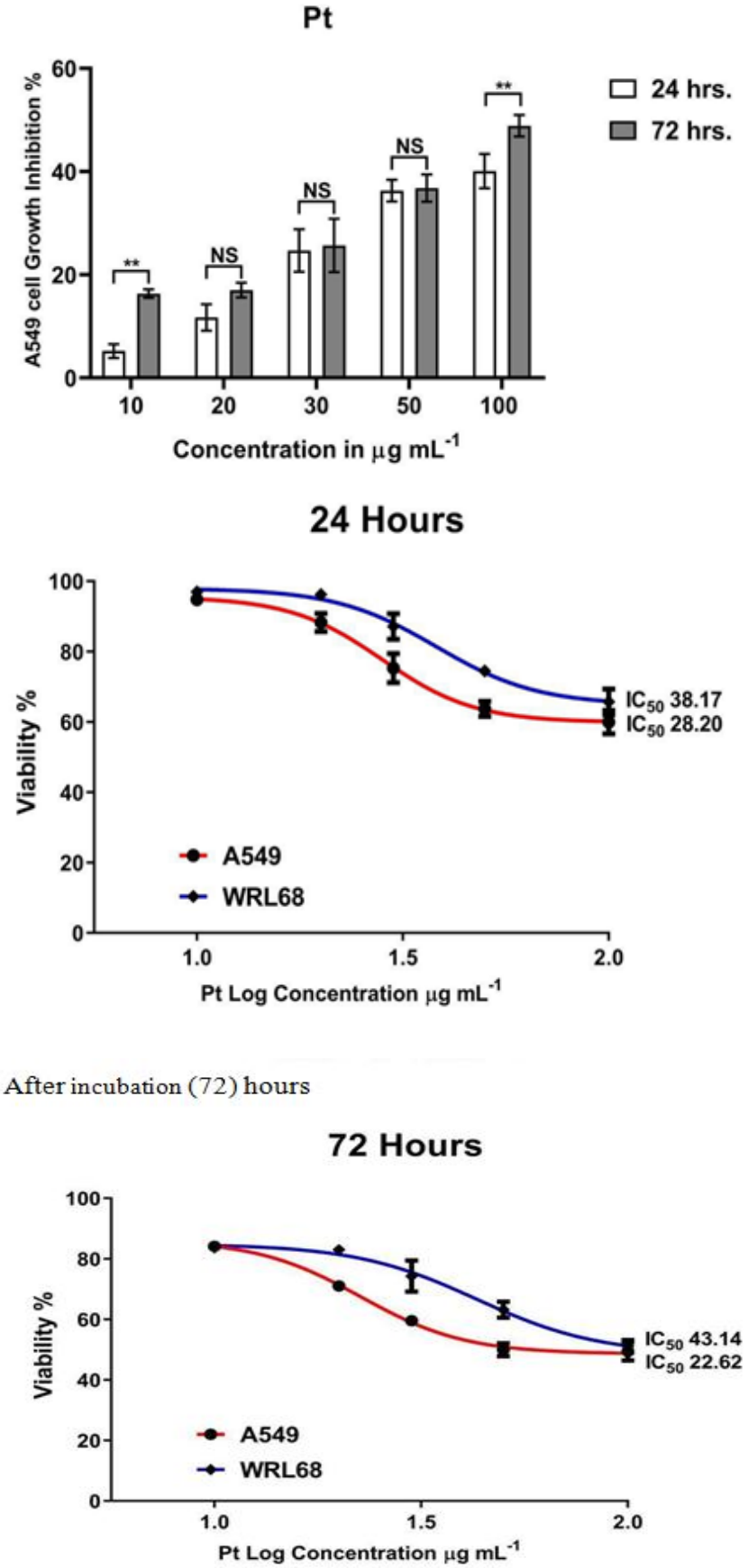

Figure (27) cytotoxicity effect of $[pt(SNT)_2Cl_2]Cl_2.H_2O$ on A_{549} cancer cell line and WRL-68 cell line after incubation (24 and 72 hours)

Annals of R.S.C.B., ISSN:1583-6258, Vol. 25, Issue 4, 2021, Pages. 7968 - 8006
Received 05 March 2021; Accepted 01 April 2021.

Table (15) Evaluation of cytotoxicity of $[pd(SNT)_2Cl_2]Cl_2.H_2O$ against A_{549} cancer cell line after incubation (24 hours) at ($37C^o$) and WRL-68 cell line

Cell line	Concentration (Mg/ml)					Number of values	IC 50 Mg/ml	p-value
	10	20	30	50	100			
A_{549}	72.801 ∓0.904	59.568 ∓ 0.821	50.000 ∓ 1.335	43.634 ∓ 2.349	39.043 ∓ 3.773	3	20.00	<0.001
WRL-68	94.830 ∓0.971	94.946 ∓ 0.998	84.336 ∓ 2.663	73.225 ∓ 1.205	64.622 ∓ 1.969	3	37.19	

After incubation (72 hours) at ($37C^o$) and WRL-68 cell line

Cell line	Concentration (Mg/ml)					Number of values	IC 50 Mg/ml	p-value
	10	20	30	50	100			
A_{549}	63.233 ∓ 1.395	51.235 ∓ 2.956	37.384 ∓ 3.457	30.710 ∓ 1.270	25.617 ∓ 1.301	3	23.27	<0.001
WRL-68	83.835 ∓ 1.142	84.143 ∓ 0.644	74.460 ∓ 5.595	660127 ∓ 2.445	50.424 ∓ 5.366	3	52.48	

Annals of R.S.C.B., ISSN:1583-6258, Vol. 25, Issue 4, 2021, Pages. 7968 - 8006
Received 05 March 2021; Accepted 01 April 2021.

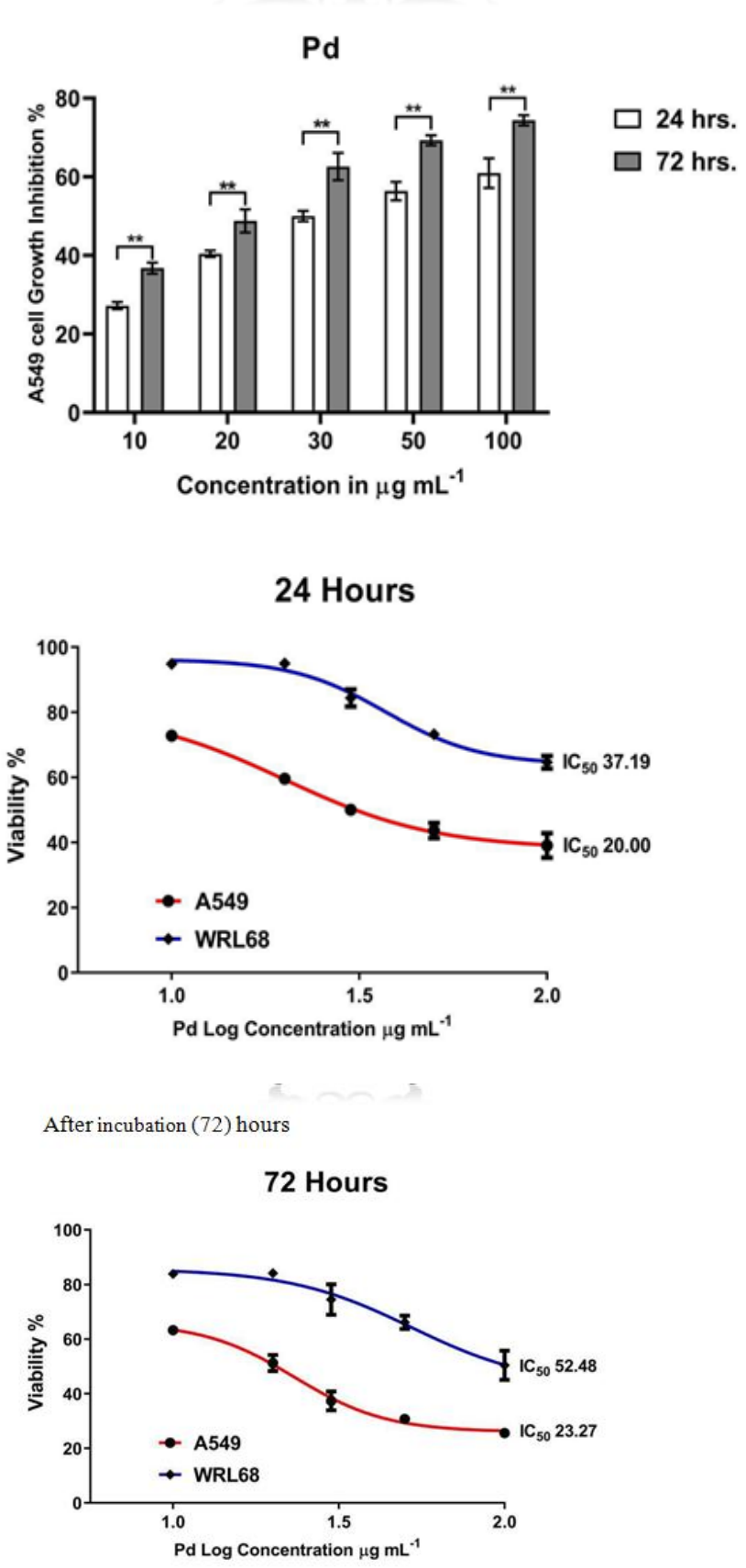

Figure(28) cytotoxicity effect of $[pd(SNT)_2Cl_2]Cl_2.H_2O$ on A_{549} cancer cell line and WRL-68 cell line after incubation (24 and 72 hours)

Annals of R.S.C.B., ISSN:1583-6258, Vol. 25, Issue 4, 2021, Pages. 7968 - 8006
Received 05 March 2021; Accepted 01 April 2021.

12-Dying performance

The quality of any fabric is directly attached on the quality of the fabric utilized to manufacture the product. More maximize dyeing procedure capacity and color performance properties [45]. The fabric fibers involved must be as clean as possible . The main target of preparation is the elimination of both naturally occurring impurities and those which are added during yarn or textile manufacturing [46]. the dying opration can be perfected on textile fabrics , yarns fabrics or garments according to the properties or for cost control .Dyes are the chemicals that are absorbed into the molecular structure of fibricfibris , which produce the color of. The molecular structure of fibric fibers. As well As is the opration which places the dyes inside the fibric fibers. the dyeing tools is used to control the necessary parameters of the dying opration in order to maximized dyeing productivity and quality [47] .

In our research cotton fabries were used for dyeing the ligand (SNT) and its complexes. The color of cotton fabrics after dying with these compound were ranged between yellow , pink ,green . As the azo compounds are considered effective dyes , which contain one or two groups that have the ability to bonded with the oxegen atom of hydroxyl group in cellulose which is the main component of cotton and all dyeing processes from

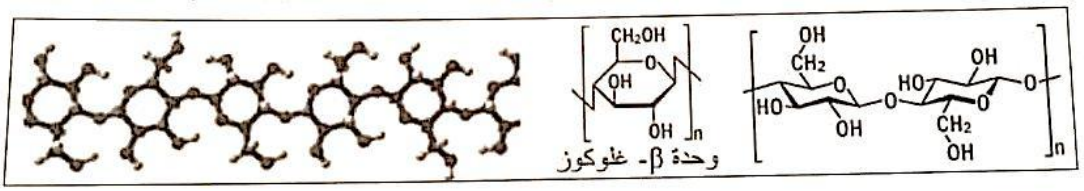

bleaching and dying. Structure of Cellulose [48]

In order to know the most important properties of the synthesized dyes, investigative studies were conducted as follows :

wash fastness

The wash fasness of synthesized ligand (SNT) and its complexes were examined depending on the (ISOO IOS CC6C25) With standard soup (SDC) [49] .

The results we a btained for all compounds were excellent. As previously mentioned because of the presence of many active groups in the composition of the compounds which helps the strength of the bonded between the dye and cotton fabrics cellulose .

Thermal stability

As Previously mentioned thermal stability has beestudied represented TGA and DSC . All the synthesized compounds have high stability in high temperature .

Photo stability

The photo stability study of the ligand (SNT) and its complexes was carried out by taking an ethanolic solution of them in a concentration (10^{-4}M) and irradiation them with (UV) rays for period (2hours) at room temperature all results were collected in Table(17) and the photo stability was calculated as the ratio to difference between the initial absorbance. i.e. before irradiation and the final, to the intial absorbance The coalition was follow

$[Cu(SNT)_2Cl_2]$>$[Ni\ (SNT)_2Cl_2]$ > $[Pd(SNT)_2]Cl_2\ .H_2O$ > $[Pt(SNT)_2Cl_2]Cl_2.\ H_2O]$>SNT

Annals of R.S.C.B., ISSN:1583-6258, Vol. 25, Issue 4, 2021, Pages. 7968 - 8006
Received 05 March 2021; Accepted 01 April 2021.

$[Ni(SNT)_2Cl_2]$

$[Pt(SNT)_2Cl_2]Cl_2.H_2O$

SNT

$[Pd(SNT)_2]Cl_2 .H_2O$

$[Cu(SNT)_2Cl_2]$

Table (17) photo degradation details of ligand and its complexes under irradiation (λ =256 nm, power = 250w)

Com pound	Time (sec)	Abs (nm)	Photo – stability percent
SNT	0	3.974	1.48%
	10	3.919	
	30	4.000	
	60	3.914	
	120	3.915	
$[Ni(SNT)_2Cl_2]$	0	3.979	5.60%
	10	3.900	
	30	3.938	
	60	3.960	
	120	3.756	
$[Pd(SNT)_2]Cl_2 .H_2O$	0	3.985	3.98%
	10	3.973	
	30	9.953	
	60	3.977	
	120	3.826	
$[Cu(SNT)_2Cl_2]$	0	0.625	7.22%
	10	0.603	
	30	0.597	
	60	0.588	
	120	0.578	
$[Pt(SNT)_2Cl_2]Cl_2.H_2O$	0	0.627	3.703
	10	0.621	
	30	0.620	

Annals of R.S.C.B., ISSN:1583-6258, Vol. 25, Issue 4, 2021, Pages. 7968 - 8006
Received 05 March 2021; Accepted 01 April 2021.

	60	0.616
	120	0.604

13-Conclusion

Ni(II) pd (II), pt (IV) and Cu (II) complexes of (SNT) ligand were synthesized . It was performed asN,N-bidentate coordinates. The geometry of Ni (II) and pt (IV) complexes are assumed octahedral while pd (II) complexes has square planar geometry and Cu (II) complexes has distorted octahedral geometry based on the available data from the spectroscopy has (FT - IR, UV –Vis, HNMR) Spectra, elemental analysis, molar conductivity, magnetic susceptibility, TGA, DSC and SEM The antibacterial, anticancer assay and dye performance were investigated .

Reference

1- Fustero, S., Sanchez-Rosello, M., Barrio, P., & Simon-Fuentes,: a fruitful decade for the synthesis of pyrazoles. *Chemical reviews*, A.) *111*(11), (2011). From (2000)to mid(2010 6984-7034.

2- Combes, R. D., &Haveland-Smith, R. B. A review of the genotoxicity of food, drug and cosmetic colours and other azo, triphenylmethane and xanthene dyes. *Mutation Research/Reviews in genetic toxicology*, *98*(2), (1982).101-243.

3- Matsui, M., Suzuki, M., Hayashi, M., Funabiki, K., Ishigure, Y., Doke, Y., &Shiozaki, H. Survey of enhanced, thermally stable, and soluble second-order nonlinear optical azochromophores. *Bulletin of the Chemical Society of Japan*, *76*(3), (2003).607-612.

4- Al-Adilee, K., &Kyhoiesh, H. A.. Preparation and identification of some metal complexes with new heterocyclic azo dye ligand 2-[2−-(1-Hydroxy-4-Chloro phenyl) azo]-imidazole and their spectral and thermal studies. *Journal of Molecular Structure*, *1137*, (2017) 160-178.

5- Nejati, K., Rezvani, Z., &Seyedahmadian, M. The synthesis, characterization, thermal and optical properties of copper, nickel, and vanadyl complexes derived from azo dyes. *Dyes and Pigments*, *83*(3), (2009). 304-311.

6- Abdu-Allah, H. H., El-Shorbagi, A. N., Abdel-Moty, S. G., El-Awady, R., & Abdel-Alim, A. A. 5-Aminosalyclic acid (5-ASA): a unique anti-inflammatory salicylate. *Med Chem (Los Angeles)*, *6*,(2016). 306-315.

7-Jarrahpour, A. A., Motamedifar, M., Pakshir, K., Hadi, N., &Zarei, M. Synthesis of novel azo Schiff bases and their antibacterial and antifungal activities. *Molecules*, *9*(10), (2004).815-824.

8- Okasha, R. M., Alsehli, M., Ihmaid, S., Althagfan, S. S., El-Gaby, M. S., Ahmed, H. E., &Afifi, T. H. First example of Azo-Sulfa conjugated chromene

moieties: Synthesis, characterization, antimicrobial assessment, docking simulation as potent class I histone deacetylase inhibitors and antitumor agents. *Bioorganic chemistry*, *92*, (2019).103262.

9- Dembitsky, V. M., Gloriozova, T. A., &Poroikov, V. V. Pharmacological and predicted activities of natural azo compounds. *Natural products and bioprospecting*, *7*(1), (2017).151-169.

10- Peterson, F. J., Holtzman, J. L., Crankshaw, D. A. U. N. E., & Mason, R. P. Two sites of azo reduction in the monooxygenase system. *Molecular pharmacology*, *34*(4), (1988).597-603.

11- Van, N., Alabada, R., Volyanskii, O. V., Koval, O. V., Kuznetsov, D. N., &Karavaeva, E. B. Novel metal complexes of bispyrazoleazo dyes for chemical fibers. *Fibre Chemistry*, *47*(6), (2016). 497-500.

12- Türker, L. Comparative Approach to Interaction of Zinc Dication with Theobromine and Theophilline-A DFT Treatment. *Earthline Journal of Chemical Sciences*, *5*(2), (2021).295-306.

13- Madhu, P. P., Prashant, G. M., Sushanth, V. H., Imranulla, M., Vivek, H. P., & Nair, A. R. THEOBROMINE: A BOON TO DENTISTRY. *INDIAN DENTAL JOURNAL* Vol. 10, (2018)

14-Georgieva, M., Kondeva-Burdina, M., Mitkov, J., Tzankova, V., Momekov, G., &Zlatkov, A. Determination of the Antiproliferative Activity of New Theobromine Derivatives and Evaluation of Their In Vitro Hepatotoxic Effects. *Anti-Cancer Agents in Medicinal Chemistry (Formerly Current Medicinal Chemistry-Anti-Cancer Agents)*,*16*(7), (2016).925-932.

15-Robertson, D. L. *Procyanidin oligomers and polyphenol oxidase: Methods for extraction optimization, enzymatic inhibition, and application as a natural inhibitor*. University of California, Davis, ProQuest Dissertations Publishing, (2010). 1477104.

Annals of R.S.C.B., ISSN:1583-6258, Vol. 25, Issue 4, 2021, Pages. 7968 - 8006
Received 05 March 2021; Accepted 01 April 2021.

16-Schimpl, F. C., Kiyota, E., Mayer, J. L. S., de CarvalhoGonçalves, J. F., da Silva, J. F., &Mazzafera, P. Molecular and biochemical characterization of caffeine synthase and purine alkaloid concentration in guarana fruit. *Phytochemistry*, *105*, (2014). 25-36.

17- Gunasekaran, S., Sankari, G., &Ponnusamy, S. Vibrational spectral investigation on xanthine and its derivatives—theophylline, caffeine and theobromine. *SpectrochimicaActa Part A: Molecular and Biomolecular Spectroscopy*, *61*(1-2), (2005). 117-127.

18- Gans, J. H. Comparative toxicities of dietary caffeine and theobromine in the rat. *Food and chemical toxicology*, *22*(5), (1984). 365-369.

19-Kim, Seo-Yul, "Observation of olefin/paraffin selectivity in Azo compound and its application into a metal–organic framework." ACS applied materials & interfaces 10.32 (2018): 27521-27530.

20-Cui, Ganglong, Pei-Jie Guan, and Wei-Hai Fang. "Photoinduced proton transfer and isomerization in a hydrogen-bonded aromatic azo compound: a CASPT2//CASSCF study." The Journal of Physical Chemistry A 118.26 (2014): 4732-4739.

21-Abbas, AlyaaKhider. "Synthesis, Spectral and Antibacterial Studies of New 1-(4-Antipyrine azo)-2-hydroxy-3, 6-Disulphonic Acid Sodium Salt with Group IIB Metal ions." Journal of Global forma Technology11(4) (2019):375-382.

22-Zhao, Rui. "One step synthesis of azo compounds from nitroaromatics and anilines." Tetrahedron letters 52.29 (2011): 3805-3809.

23-Abbas, AlyaKhider, and Rafal Salam Kadhim. "Metal Complexes of Proline-Azo Dyes, Synthesis, Characterization, Dying Performance and Antibacterial Activity Studies." Orient J Chem 33 (2017): 402-417.

24-AbouEl-Enein, Saeyda A. "Synthesis and characterization of some metal complexes derived from azo compound of 4, 4′-methylenedianiline and antipyrine: evaluation of their biological activity on some land snail species." Journal of Molecular Structure 1099 (2015): 567-578

25-Smorra, C. "A parts-per-billion measurement of the antiproton magnetic moment." Nature 550.7676 (2017): 371-374.

26-Nyquist, Richard A., and Ronald O. Kagel. Handbook of infrared and raman spectra of inorganic compounds and organic salts: infrared spectra of inorganic compounds. Vol. 4. Academic press, 2012.

27-Gup, Ramazan, EmrahGiziroglu, and BülentKırkan. "Synthesis and spectroscopic properties of new azo-dyes and azo-metal complexes derived from barbituric acid and aminoquinoline." Dyes and pigments 73.1 (2007): 40-46

28-Popescu, Liviana, "Study of thermally induced interactions between theobromine and various sweeteners." Journal of Thermal Analysis and Calorimetry 138.3 (2019): 2347-2356.

29-Khanmohammadi, Hamid, and Maryam Darvishpour. "New azo ligands containing azomethine groups in the pyridazine-based chain: synthesis and characterization." Dyes and Pigments 81.3 (2009): 167-173

30-Karcı, Fikret. "Synthesis of 4-amino-1H-benzo [4, 5] imidazo [1, 2-a] pyrimidin-2-one and its disperse azo dyes. Part 1: Phenylazo derivatives." Dyes and Pigments 71.2 (2006): 90-96.

31-Dinçalp, Haluk, et al. "New thiophene-based azo ligands containing azomethine group in the main chain for the determination of copper (II) ions." Dyes and Pigments 75.1 (2007): 11-24.

32-Men, Yana . "Tailoring the electronic structure of Co2P by N doping for boosting hydrogen evolution reaction at all pH values." ACS Catalysis 9.4 (2019): 3744-3752

33-Al-Hamdani, Abbas Ali Salih, and Rehab GhalibHamoodah. "Transition metal complexes with tridentate ligand: preparation, spectroscopic characterization, thermal analysis and structural studies." Baghdad Science Journal 13.4 (2016).

34-Al-Adilee, Khalid J., Khamis A. Abedalrazaq, and ZainabMohsin Al-Hamdiny. "Synthesis and spectroscopic properties of some transition metal complexes with new azo-dyes derived from thiazole and imidazole." Asian Journal of Chemistry 25.18 (2013): 10475.

35-Gaber, Mohamed, Nadia El-Wakiel, and Osama M. Hemeda. "Cr (III), Mn (II), Co (II), Ni (II) and Cu (II) complexes of 7-((1H-benzo [d] imidazol-2-yl) diazenyl)-5-nitroquinolin-8-ol. synthesis, thermal, spectral, electrical measurements, molecular modeling and biological activity." Journal of Molecular Structure 1180 (2019): 318-329.

36-El-Ghamry, Hoda A., Shaimaa K. Fathalla, and Mohamed Gaber. "Synthesis, structural characterization and molecular modelling of bidentateazo dye metal complexes: DNA interaction to antimicrobial and anticancer activities." Applied Organometallic Chemistry 32.3 (2018): e4136.

37-Schweiger, Martin J., and Wolfgang Beck. "Metal Complexes of Biologically Important Ligands, Part CLXXVIII. Addition of the PentacarbonylrheniumCation [(OC) 5Re]+ to the Xanthine Alkaloids Caffeine, Theophylline, and Theobromine." Zeitschriftfüranorganische und allgemeineChemie 643.21 (2017): 1335-1337.

38-Jain, Reena, Rajeev Singh, and N. K. Kaushik. "Synthesis, characterization, and thermal and antimicrobial activities of some novel organotin (IV): Purine base complexes." Journal of Chemistry 2013 (2013).

39-Iftikhar, Bushra. "Synthesis, characterization and biological assay of Salicylaldehyde Schiff base Cu (II) complexes and their precursors." Journal of Molecular Structure 1155 (2018): 337-348.

40-Jadou, BushraKamel, Ali JamilHameed, and Ali Zayed Al-Rubaie. "Synthesis, Antimicrobial, Antioxidant and Structural Studies of Some New Sulfa Drug Containing an Azo-azomethine Group." Egyptian Journal of Chemistry 64.2 (2021): 751-759.

41-Liu, Yongchun. "Palladium-based nanomaterials for cancer imaging and therapy." Theranostics 10.22 (2020): 10057.

42-Carneiro, Tatiana J. "Metabolic Aspects of Palladium (II) Potential Anti-Cancer Drugs." Frontiers in oncology 10 (2020): 2218.

43-Brabec, Viktor. "Valuable insight into the anticancer activity of the platinum-histone deacetylase inhibitor conjugate, cis-[Pt (NH3) 2malSAHA–2H)]." Molecular pharmaceutics 9.7 (2012): 1990-1999.

44-Yang, Jun. "Conjugate of Pt (IV)–histone deacetylase inhibitor as a prodrug for cancer chemotherapy." Molecular pharmaceutics 9.10 (2012): 2793-2800.

45-Al-Majidi, Suaad MH, and Mohammed GA Al-Khuzaie. "Synthesis and Characterization of New Azo Compounds Linked to 1, 8-Naphthalimide and Studying Their Ability as Acid-Base Indicators." Iraqi Journal of Science (2019): 2341-2352.

46-Al-Khuzaie, Mohammed GA, and Suaad MH Al-Majidi. "Synthesis and characterization of new azo compounds linked to 1, 8-naphthalimide as new fluorescent dispersed dyes for cotton fibers." Journal of Physics: Conference Series. Vol. 1664. No. 1. IOP Publishing, 2020.

Annals of R.S.C.B., ISSN:1583-6258, Vol. 25, Issue 4, 2021, Pages. 7968 - 8006
Received 05 March 2021; Accepted 01 April 2021.

47-Memon, Hafeezullah, N. Ali Khoso, and SamiullahMemon. "Effect of dyeing parameters on physical properties of fibers and yarns." International Journal of Applied Sciences and Engineering Research 4.4 (2015): 401-407.

48-Ullah, Muhammad Wajid. "Synthesis, structure, and properties of bacterial cellulose." Nanocellulose: From Fundamentals to Advanced Materials (2019): 81-113.

49-Kant, Rita. "Textile dyeing industry an environmental hazard." (2011).